



Contents lists available at ScienceDirect

## Bioorganic &amp; Medicinal Chemistry

journal homepage: [www.elsevier.com/locate/bmc](http://www.elsevier.com/locate/bmc)

## 5-Substituted 3-chlorokenpaullone derivatives are potent inhibitors of *Trypanosoma brucei* bloodstream forms

Oliver C. F. Orban<sup>a,†</sup>, Ricarda S. Korn<sup>a,†</sup>, Diego Benítez<sup>b</sup>, Andrea Medeiros<sup>b,c</sup>, Lutz Preu<sup>a</sup>, Nadège Loaëc<sup>d</sup>, Laurent Meijer<sup>d</sup>, Oliver Koch<sup>e</sup>, Marcelo A. Comini<sup>b,\*</sup>, Conrad Kunick<sup>a,f,\*</sup>

<sup>a</sup> Technische Universität Braunschweig, Institut für Medizinische und Pharmazeutische Chemie, Beethovenstraße 55, D-38106 Braunschweig, Germany

<sup>b</sup> Group Redox Biology of Trypanosomes, Institut Pasteur de Montevideo, Matajojo 2020, CP 11400 Montevideo, Uruguay

<sup>c</sup> Departamento de Bioquímica, Facultad de Medicina, Universidad de la República, Gral. Flores 2125, Montevideo, Uruguay

<sup>d</sup> ManRos Therapeutics, Perharidy Research Center, 29680 Roscoff, France

<sup>e</sup> Faculty of Chemistry and Chemical Biology, TU Dortmund University, Otto-Hahn-Straße 6, 44227 Dortmund, Germany

<sup>f</sup> Technische Universität Braunschweig, Center of Pharmaceutical Engineering (PVZ), Franz-Liszt-Straße 35A, D-38106 Braunschweig, Germany

## ARTICLE INFO

## Article history:

Received 11 April 2016

Revised 9 June 2016

Accepted 11 June 2016

Available online xxxx

## Keywords:

Leishmaniasis

Neglected tropical diseases

Paullone

Trypanosomiasis

Trypanothione synthetase

*Trypanosoma brucei*

## ABSTRACT

Trypanothione synthetase is an essential enzyme for kinetoplastid parasites which cause highly disabling and fatal diseases in humans and animals. Inspired by the observation that *N*(5)-substituted paullones inhibit the trypanothione synthetase from the related parasite *Leishmania infantum*, we designed and synthesized a series of new derivatives. Although none of the new compounds displayed strong inhibition of *Trypanosoma brucei* trypanothione synthetase, several of them caused a remarkable growth inhibition of cultivated *Trypanosoma brucei* bloodstream forms. The most potent congener **3a** showed antitrypanosomal activity in double digit nanomolar concentrations and a selectivity index of three orders of magnitude versus murine macrophage cells.

© 2016 Elsevier Ltd. All rights reserved.

## 1. Introduction

Of the seventeen 'neglected tropical diseases' designated by the World Health Organization, three groups of infectious diseases (Human African trypanosomiasis, Chagas disease, and Leishmaniasis) are caused by hemoflagellated parasites belonging to the family *Trypanosomatidae*.<sup>1</sup> The Human African Trypanosomiasis (HAT, also called sleeping sickness) is caused by *Trypanosoma brucei* par-

asites which are injected by tsetse flies during a blood meal. Without proper treatment, the infection is fatal in its final stage. Chagas disease is a life-threatening infection caused by *Trypanosoma cruzi* which is transmitted through contact with biting triatomine bugs. The different forms of leishmaniasis are caused by parasites of various *Leishmania* species which use biting female sandflies as vectors. The most dangerous form is visceral leishmaniasis (VL). It affects internal organs, a deadly situation if patients do not receive a proper medication.<sup>1</sup> While all these infections occur in different forms and stages, they have in common that mainly the poverty-stricken population in tropical and subtropical areas of the third world is affected and that they may lead to serious impairment of body functions or a fatal outcome if left untreated. The number of drugs available for a curative treatment of these infections is rather limited, with most of them suffering from serious shortcomings such as high costs, long treatment periods, complicated application procedures, need for hospitalization, or severe side effects. Moreover, in some areas parasites have developed resistance against drugs that have been successfully used for treatment over decades, the most prominent example being the resistance of *Leishmania* parasites against pentavalent antimonials in the

**Abbreviations:** ACN, acetonitrile; CDK, cyclin-dependent kinase; CLK, cdc2-like kinase; CK, casein kinase; DIPEA, diisopropylethylamine; DMEM, Dulbecco's modified Eagle's medium; DMF, *N,N*-dimethylformamide; DMSO, dimethyl sulfoxide; DYRK1A, dual specificity tyrosine phosphorylation-regulated protein kinase 1A; DTT, dithiothreitol; EDTA, ethylenediaminetetraacetic acid; EGTA, ethylene glycol-bis(β-aminoethyl ether)-*N,N,N',N'*-tetraacetic acid; FCS, fetal calf serum; FSC, forward scatter; GSK-3, glycogen synthase kinase-3; HEPES, 4-(2-hydroxyethyl)-1-piperazineethanesulfonic acid; PyBOP, benzotriazol-1-yl-oxytripyrrolidinophosphonium-hexafluorophosphate; SSC, side scatter; SD, standard deviation; THF, tetrahydrofuran; TryS, trypanothione synthetase.

\* Corresponding authors. Tel.: +598 25220910 (M.A.C.), +49 5313912751 (C.K.).

E-mail addresses: [mcomini@pasteur.edu.uy](mailto:mcomini@pasteur.edu.uy) (M.A. Comini), [c.kunick@tu-braunschweig.de](mailto:c.kunick@tu-braunschweig.de) (C. Kunick)

† Co-first authors.

<http://dx.doi.org/10.1016/j.bmc.2016.06.023>

0968-0896/© 2016 Elsevier Ltd. All rights reserved.

province Bihar in India.<sup>2,3</sup> Despite the fact that leishmaniasis and trypanosomiasis account for 2 million new cases of infection per year, the development of new drugs is unlikely to be profitable, since most affected patients are unable to afford expensive new medicines. Nevertheless, to overcome problems with emerging resistances and safety issues, the development of novel efficacious and safer drugs against *Trypanosoma* and *Leishmania* infections is urgently needed.<sup>4,5</sup> In order to avoid cross-resistance with established medications, the novel drugs should represent new chemotypes and target novel and indispensable parasite's biomolecules. In this respect, the thiol-redox metabolism of trypanosomatids offers unique opportunities for a selective and efficacious impairment of pathogen's viability. In *Trypanosomatidae* parasites, the dithiol trypanothione (bis-glutathionylspermidine) substitutes glutathione as major redox co-substrate that supports the intracellular redox homeostasis providing protection against oxidative stress and reducing equivalents for the biosynthesis of nucleic acids. The enzyme trypanothione synthetase (TryS) synthesizes trypanothione by ATP-dependent conjugation of spermidine with two molecules of glutathione (Fig. 1).<sup>6–12</sup>

Details of the chemical mechanisms catalyzed by TryS have been reported.<sup>13–15</sup> TryS has been suggested as chemotherapeutic target against trypanosomatid parasites based on its demonstrated indispensability for *T. brucei*<sup>16–18</sup> and *L. infantum*<sup>19</sup> and the complete lack of homologue sequences in the human host. Recently, *N*(5)-substituted paullones were identified as inhibitors of TryS.<sup>19,20</sup>

Paullones (Chart 1) are a group of 7,12-dihydroindolo[3,2-*d*][1]benzazepin-6(5*H*)-ones which besides other biological properties<sup>21–23</sup> display inhibitory activities against mammalian protein kinases of the CMGC superfamily, e.g., cyclin-dependent kinases (CDKs)<sup>24–26</sup> and glycogen synthase kinase-3 (GSK-3).<sup>27,28</sup> Kenpaullone (**1a**),<sup>29</sup> the prototype of the series, is used as a standard GSK-3 inhibitor which displays selectivity versus a wide array of protein kinases (e.g., ERK1, DYRK1A, VEGF-R2, PLK1, INS-R).<sup>30,31</sup> Of note, paullones bind to the ATP binding site of kinases via the nitrogen atom in 5-position which acts as hydrogen bond donor.<sup>32</sup> In consequence, *N*(5)-substituted paullones lose the kinase inhibitory activity.<sup>33</sup>

Moreover, previous studies involving paullones as anti-TryS scaffolds revealed that substitution of 4-azapaullones in position 9 or 11 with alkyl or aryl groups is detrimental for target inhibition<sup>34</sup>, whereas paullones harboring a methyl ethylenediamine side

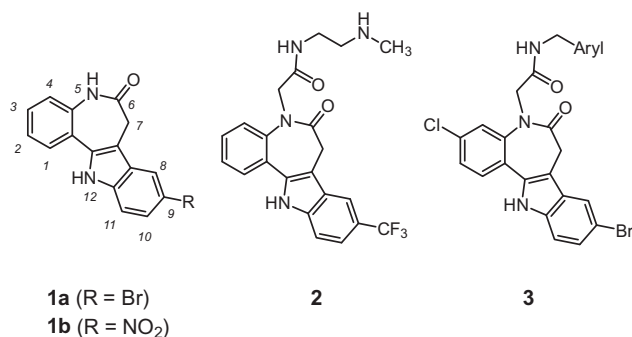


**Chart 1.** Paullones mentioned in the text: kenpaullone (**1a**), alsterpaullone (**1b**), FS-554 (**2**), and title compounds **3**.

chain at the *N*(5)-position (e.g., **2**) inhibited both recombinant *L. infantum* TryS (*Li*TryS) and the in vitro growth of *L. infantum* promastigotes (insect stage).<sup>19,20</sup> The most potent derivative (IC<sub>50</sub> 0.15 μM and EC<sub>50</sub> 12 μM), containing halogen substituents in position 3 (chloro) and 9 (bromo), produced a significant depletion of trypanothione in *L. infantum*, which confirmed its on-target effect.<sup>19,20</sup> We here report an approach to develop new paullones with potent growth inhibitory activity against the infective form of *T. brucei*. The new compounds were also screened for their anti-TryS activity against the enzyme from three major pathogenic species of trypanosomatids: *T. brucei*, *T. cruzi* and *L. infantum*.

## 2. Drug design and synthesis

The *N*(5)-substituted paullone FS-554 (**2**) inhibited very selectively recombinant *Li*TryS but only moderately the trypanosomal TryS. Here we employed a structure-based rational approach aimed to design novel paullones with increased TryS inhibitory activity and a concomitant selective anti-parasitic activity. A model of *Leishmania major* TryS (*Lm*TryS) with mechanistically important regions involved in substrate (ATP) binding was previously generated.<sup>13</sup> Analysis of the binding mode of ATP to *Lm*TryS revealed that it is located in a large and solvent accessible pocket, anchored by a double hydrogen bond motif between the aminopyrimidine substructure and the backbone amide groups of Gln583 and Phe585 of the protein. This hydrogen bonding pattern to an extended part of the protein chain shows a high similarity to the

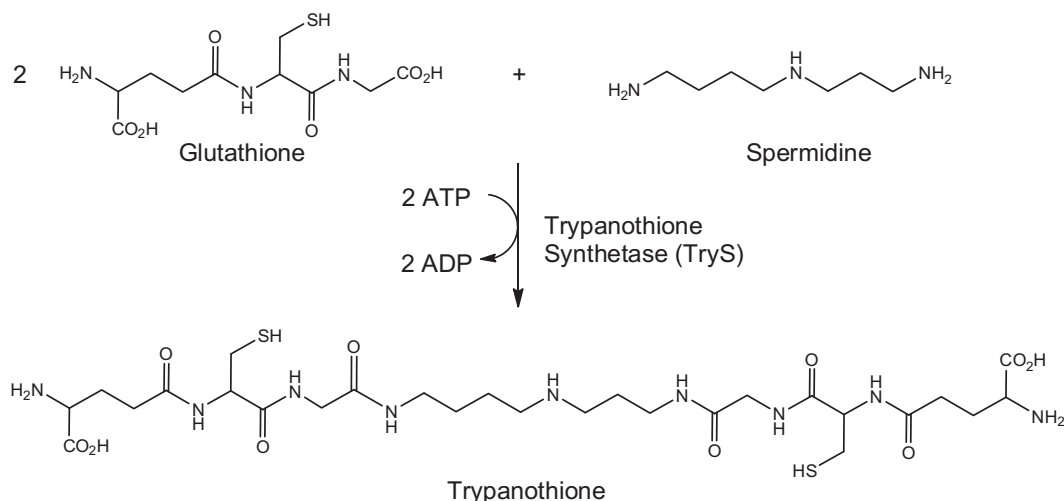


**Figure 1.** Synthesis of trypanothione from spermidine and glutathione by trypanothione synthetase (TryS). The reaction is a two-step process, of which both steps are reversible by the action of an amidase activity located in the N-terminal domain of TryS. ATP is necessary to activate glutathione by phosphorylation of the glycine carboxylate function. Modified from Ref. 13.

interaction of the well-known hinge region of protein kinases to both ATP and ATP-competitive kinase inhibitors.<sup>35</sup>

Figure 2 shows a comparison between a TryS model containing FS-554 (**2**) and a crystal structure of the mammalian kinase GSK-3 in complex with alsterpaullone (**1b**). *LmTryS* and GSK-3 show a high structural and sequence similarity within the ATP binding site (see Fig. 2b). Based on this similarity FS-554 (**2**) was modeled into the *LmTryS* structure using the binding mode of alsterpaullone (**1b**) to GSK-3 as template. The resulting model can be used to find a possible explanation of the different activities of paullone scaffolds. FS-554 does not show any kinase inhibitory activity since the characteristic hydrogen bond pattern to the hinge region of the kinase found with *N*(5)-unsubstituted paullones like alsterpaullone is hampered by the *N*(5) side chain in FS-554. In the GSK-3 structure, this side chain leads to a steric clash of FS-554 with Tyr134 of the hinge region (see Fig. 2b). In contrast, the *LmTryS* structure shows a cleft at the corresponding TryS ‘hinge region’, where the *N*(5) side chain of FS-554 can be accommodated. Moreover, in TryS the side chain amide of FS-554 can form a

hydrogen bonding interaction to the backbone carbonyl group of Phe586 that is slightly moved upwards in contrast to the corresponding kinase hinge region which points into the ATP binding site. Interestingly, the methylaminoethyl part is placed near a hydrophobic region of Leu585. Because the *N*(5) side chain is needed for selective TryS inhibition on the one hand and an extension of the hydrophobic part in this area can lead to a gain of affinity on the other hand, we designed the series **3** by replacing the methylaminoethyl chain of **2** by benzyl or heteroarylmethyl moieties to increase the hydrophobic interaction potential between ligand and protein.

The *N*(5)-substituted paullones **3a–l** were prepared from 3-chlorokenpaullone **8** as central building block (Scheme 1). Although innovative new paullone syntheses catalyzed by transition metals have been reported lately,<sup>36–39</sup> we prepared **8** by a traditional acid-induced Fischer indolization procedure<sup>40</sup> for the sake of simplicity.<sup>41</sup> In brief, the synthesis of **8** started by the reaction of methyl 4-chloroanthranilate **4** with methyl succinylchloride. A subsequent Dieckmann reaction of the resulting amide **5** yielded the

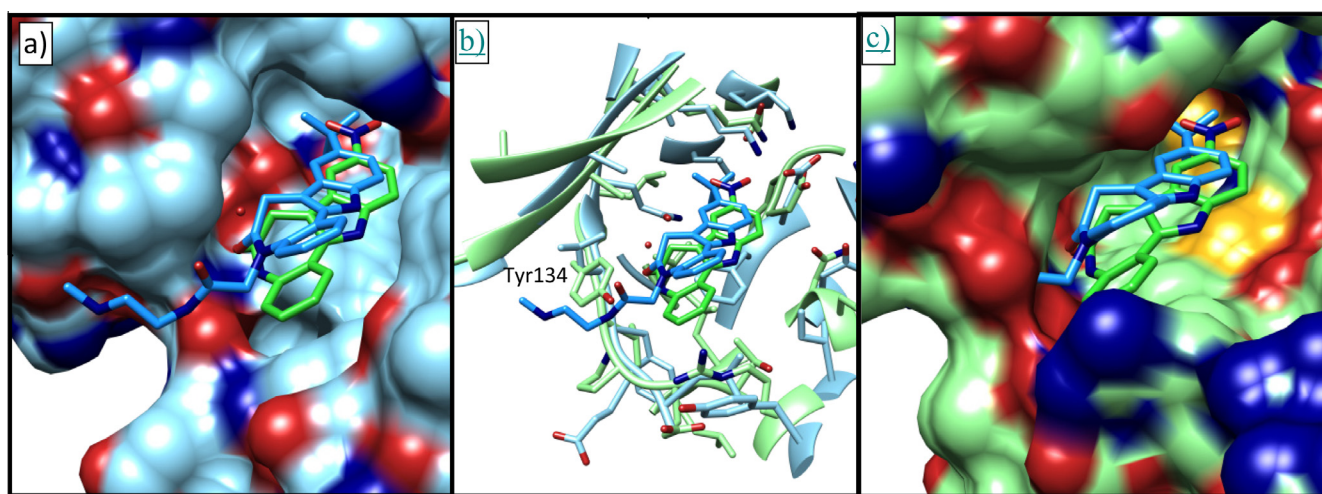
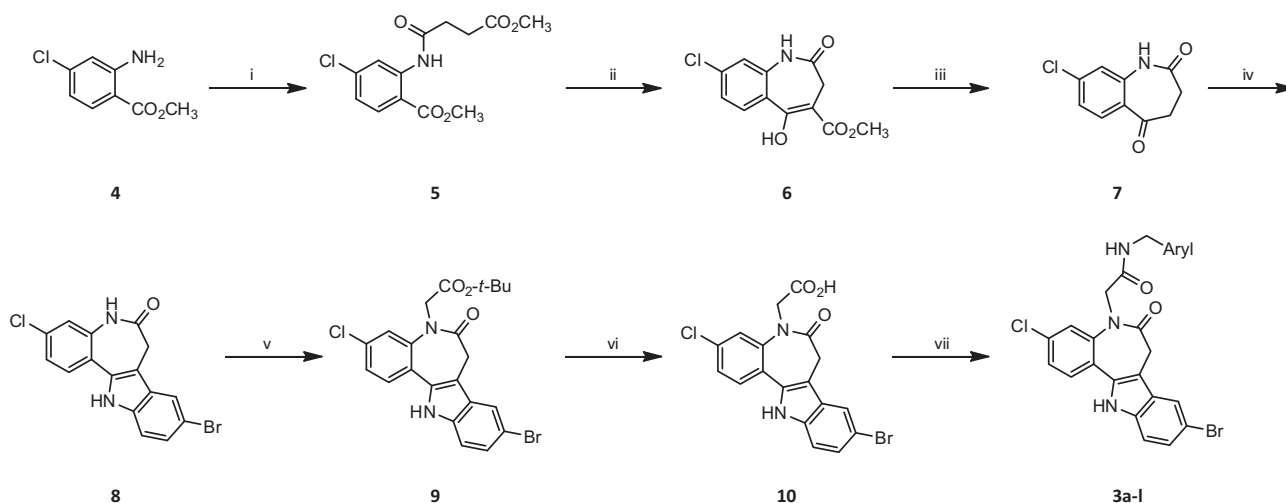


**Figure 2.** Binding mode comparison between GSK-3 (lime green surface) in complex with alsterpaullone (**1b**, green) and *LmTryS* (light blue surface) with modeled FS-554 (**2**, blue). (a) *LmTryS* surface with FS-554 and alsterpaullone. (b) Ribbon representation and important amino acid side chains with high similarity. (c) GSK-3 surface with alsterpaullone and FS-554.



**Scheme 1.** Synthesis of *N*(5)-substituted 3-chlorokenpaullones **3a–l**. For aryl substituents refer to Table 1. Reagents and conditions: (i) methyl succinyl chloride, pyridine, toluene, 0 → 80 °C, 2 h, 89%; (ii) KO<sup>t</sup>Bu, DMF, toluene, 0 → 80 °C, 3.5 h, 65%; (iii) DMSO/H<sub>2</sub>O 9:1, 150 °C, 6 h, 53%; (iv) 1. 4-bromophenylhydrazine hydrochloride, AcOH, NaOAc, 70 °C, 1 h 2. AcOH, H<sub>2</sub>SO<sub>4</sub>, 70 °C, 1 h, 41%; (v) 1. KO<sup>t</sup>Bu, THF, rt, 1 h 2. *tert*-butyl 2-bromoacetate, THF, rt, 22 h, 62%; (vi) TFA, CH<sub>2</sub>Cl<sub>2</sub>, rt, 22 h, quantitative conversion; (vii) DMF, PyBOP, DIPEA, arylmethylamines, 0 °C → rt, 20 h, 10–53%.

enolized cyclic  $\beta$ -oxocarboxylic acid ester **6** which was then dealkoxycarbonylated by heating in wet DMSO under neutral conditions. The so-prepared cyclic ketone **7** was reacted with 4-bromophenylhydrazine, yielding the 3-chlorokenpaullone **8**. A selective alkylation of **8** at *N*(5) was accomplished by deprotonation with potassium *tert*-butoxide in THF and subsequent reaction with *tert*-butyl 2-bromoacetate. Subsequently, the resulting ester **9** was deprotected by means of trifluoroacetic acid yielding 2-(3-chlorokenpaullone-5-yl)acetic acid (**10**). Eventually, the desired title compounds **3a–l** were prepared by PyBOP-promoted reaction of **10** with appropriate arylmethylamines in the presence of diisopropylethylamine (DIPEA).

### 3. Biological evaluation and discussion

The new 5-substituted compounds **3a–l** were evaluated for inhibitory activity on the TryS of three trypanosomatid parasite species: *T. brucei*, *T. cruzi*, and *L. infantum*. All compounds of series **3** and FS-554 (**2**), which was used as a standard, were tested for 15 min at an initial concentration of 30  $\mu$ M using an end point assay based on the determination of inorganic phosphate released from ATP during TryS catalysis. If more than 50% inhibition was observed,  $IC_{50}$  values were determined. The results (Table 1) show that most compounds from the new series **3** exhibit only a modest improvement of inhibitory activity over **2** towards *T. brucei* TryS (e.g., 40–60% enzyme inhibition for **3a–h** at 30  $\mu$ M versus 30% TryS inhibition for FS-554 at 30  $\mu$ M). In general, in the *N*(5) side chain terminal phenyl rings were preferred over pyridyl moieties (25–35% TryS inhibition for **3j–l**). Interestingly, with the exception of **3a**, **3j**, and **3l**, several of the new 5-substituted paullones of series **3** inhibited TryS of *T. cruzi* with  $IC_{50}$  values near 10  $\mu$ M and in this regard were superior to FS-554 ( $IC_{50} \sim 30 \mu$ M). At variance with the *T. brucei* TryS, the enzyme from *T. cruzi* displayed a higher promiscuity for the terminal aryl substituent of the *N*(5) side chain. Overall, the results obtained for the trypanosomal TryS indicate that the inclusion of a *N*(5) side chain with a terminal aryl group positively affects inhibition, albeit to different extent depending on the TryS species.

Strikingly, the situation was different for TryS of *L. infantum*. Exhibiting an  $IC_{50}$  value of 0.35  $\mu$ M, FS-554 (**2**) was in this case clearly more potent compared to all new *N*(5)-substituted paullones **3** reported in this study. The only congener with a comparable, albeit lower, activity against *L. infantum* TryS was

the 4-pyridyl compound **3j** ( $IC_{50}$  1.2  $\mu$ M). SAR analysis further revealed that an H-bond donor group (OH) at *para* position of the phenyl ring (**3h**,  $IC_{50}$  10  $\mu$ M) contributes to the inhibitory activity since 4-unsubstituted derivatives or bearing H-bond acceptors were less active (Table 1). The most potent *Li*TryS inhibitor was the aminoalkyl derivative **2** (FS-554). It harbors at *N*(5) position an ethylenediamine moiety with two nitrogen atoms that also may potentially be engaged in H-bond formation with protein residues from the active site and might explain the higher activity of this derivative. On the other hand, an additional explanation for the lower activity displayed by the new paullone derivatives **3** compared to FS-554 may lie on the fact that the aryl rings of **3** present a more rigid conformation than an alkyl chain and, thus, offer a reduced repertoire of conformers suited for proper accommodation into the active site pocket of the enzyme.

Although the rationale behind our design strategy for series **3** was not corroborated by the inhibition results for *Li*TryS, our results support the occurrence of important structural differences at the ATP-binding site of these enzymes.<sup>7,14,19</sup> Noteworthy, TryS belongs to the ATP-grasp family of proteins, which undergo important conformational changes in regions and structural elements shaping their ATP-binding site upon substrate binding. Based on this and given the high degree of sequence conservation for the ATP-binding region among trypanosomatid's TryS, it is tempting to speculate that secondary residues or elements in the active site of these enzymes play an important role in modulating the interaction with ligands. In a more general context, these data add value to a recent biochemical study with TryS from trypanosomatids performed by our groups, which proposed the existence of species-specific differences between TryS to explain the selective interaction of the enzymes with different ligands (substrates, inhibitors).<sup>20</sup>

While the tests on isolated TryS enzymes produced disappointing results, several compounds of series **3** exhibited potent antiparasitic activity on cultivated *T. brucei* bloodstream forms with single digit or submicromolar  $EC_{50}$  values. This biological activity was clearly related to the structure of the congeners, since the three compounds **3j–l** with a pyridylmethyl moiety as part of the side chain in 5-position were less potent compared to the derivatives with a benzyl structure (**3a–3i**), except for compound **3c** as discussed below. Among this subgroup the parent compound **3a**, which is unsubstituted at the phenyl ring, was tenfold more active against the parasites compared to 4- or 3-mono- or di-substituted

**Table 1**  
Biological activities and physicochemical properties of *N*(5)-substituted paullones **3**

	Aryl	<i>Tb</i> TryS activity <sup>a</sup> [%]	<i>Tc</i> TryS activity [%] or $IC_{50}$ <sup>a</sup> [ $\mu$ M]	<i>Li</i> TryS activity [%] or $IC_{50}$ <sup>a</sup> [ $\mu$ M]	Viability of <i>T. b. brucei</i> [%] or $EC_{50}$ <sup>b</sup> [ $\mu$ M]	Selectivity index <sup>c</sup>	Predicted $\log P^d$	$S_{0,exp}$ <sup>e</sup> [ $\mu$ mol/L]
<b>3a</b>	Ph	45.2 ( $\pm$ 4.1)	72.8 ( $\pm$ 5.0)%	50.0 ( $\pm$ 4.0)%	0.04 $\pm$ 0.01 $\mu$ M	1410	4.23	<0.49
<b>3b</b>	4-Cl-Ph	50.1 ( $\pm$ 7.9)	11 ( $\pm$ 2) $\mu$ M	109.1 ( $\pm$ 8.3)%	0.8 ( $\pm$ 0.2) $\mu$ M	>62	4.79	ND
<b>3c</b>	2-Cl-Ph	55.3 ( $\pm$ 8.2)	11 ( $\pm$ 3) $\mu$ M	23 ( $\pm$ 4) $\mu$ M	53.2 ( $\pm$ 4.0)%	ND	4.79	ND
<b>3d</b>	3-Cl-Ph	55.9 ( $\pm$ 6.9)	11 ( $\pm$ 2) $\mu$ M	17 ( $\pm$ 3) $\mu$ M	1.1 ( $\pm$ 0.2) $\mu$ M	$\sim$ 91	4.79	ND
<b>3e</b>	3,4-Cl <sub>2</sub> -Ph	42.0 ( $\pm$ 4.2)	9 ( $\pm$ 1) $\mu$ M	19 ( $\pm$ 3) $\mu$ M	0.84 ( $\pm$ 0.2) $\mu$ M	$\sim$ 12	5.34	ND
<b>3f</b>	4-Me-Ph	53.7 ( $\pm$ 3.6)	9 ( $\pm$ 2) $\mu$ M	48.6 ( $\pm$ 8.2)%	0.3 ( $\pm$ 0.1) $\mu$ M	>167	4.72	<0.48
<b>3g</b>	4-MeO-Ph	53.5 ( $\pm$ 3.0)	11 ( $\pm$ 4) $\mu$ M	24 ( $\pm$ 5) $\mu$ M	1 ( $\pm$ 0.3) $\mu$ M	22	4.10	ND
<b>3h</b>	4-HO-Ph	58.0 ( $\pm$ 7.2)	9 ( $\pm$ 3) $\mu$ M	10 ( $\pm$ 3) $\mu$ M	0.84 ( $\pm$ 0.2) $\mu$ M	$\sim$ 238	3.84	<4.8
<b>3i</b>	4-CF <sub>3</sub> -Ph	63.5 ( $\pm$ 7.2)	9 ( $\pm$ 2) $\mu$ M	55.4 ( $\pm$ 3.7)%	1.8 ( $\pm$ 0.3) $\mu$ M	>18	5.15	ND
<b>3j</b>	4-Pyridyl	65.2 ( $\pm$ 3.7)	58.1 ( $\pm$ 5.2)%	1.2 ( $\pm$ 0.5) $\mu$ M	49.1 ( $\pm$ 0.7)%	ND	2.89	ND
<b>3k</b>	3-Pyridyl	64.8 ( $\pm$ 4.5)	9 ( $\pm$ 3) $\mu$ M	11 ( $\pm$ 3) $\mu$ M	59.4 ( $\pm$ 2.4)%	ND	2.89	ND
<b>3l</b>	2-Pyridyl	75.8 ( $\pm$ 4.5)	54.8 ( $\pm$ 9.9)%	95.5 ( $\pm$ 3.8)%	33.8 ( $\pm$ 2.2)%	ND	3.32	ND
FS-554 ( <b>2</b> )	n.a.	70.0 ( $\pm$ 4.9)	44.5 ( $\pm$ 3.8)%	0.35 ( $\pm$ 0.5) $\mu$ M	8.3 ( $\pm$ 0.8) $\mu$ M	$\sim$ 1	1.65	ND

n.a. = not applicable.

ND = not determined.

<sup>a</sup> Residual TryS activity ( $\pm$ 2 SD) [%] at 30  $\mu$ M, or  $IC_{50}$  ( $\pm$ 2 SD) [ $\mu$ M].

<sup>b</sup> Viability of infective *T. b. brucei* ( $\pm$ SD) [%] at 5  $\mu$ M, or  $EC_{50}$  ( $\pm$ SD) [ $\mu$ M].

<sup>c</sup> Ratio  $EC_{50}$  murine macrophages/ $EC_{50}$  *T. b. brucei*.

<sup>d</sup> Calculated with ChemBioDraw Ultra, version 13.02.3021.

<sup>e</sup> Solubility determined by shake-flask-method, pH = 7.4; 25  $^{\circ}$ C; 48 h incubation time.

derivatives (**3b**, **3d–3i**). The effect was even more dramatic on 2-substitution, as the *ortho* chloro-substituted derivative **3c** was explicitly inferior to the *para* and *meta* isomers **3b** and **3d** ( $EC_{50} \sim 1 \mu\text{M}$ ). Compounds with single digit micromolar or submicromolar antitrypanosomal activity were also tested on murine macrophages. Three compounds (**3a**, **3f** and **3h**) showed a significant selectivity profile ( $SI \geq 100$ ) for the parasite cells. Although the 5-substitution at the paullone heterocyclic parent scaffold in **3a–i** should, on a structural basis, prevent any inhibition of protein kinases, the compound showing the most potent antitrypanosomal activity (**3a**) was evaluated on mammalian kinases that are typically inhibited by paullones (CDK1/cyclin B, CDK2/cyclin A, CDK5/p25, CDK9/cyclin T, GSK-3) and related kinases (CK1, CLK1, DYRK1A). **3a** failed to inhibit all protein kinases in the panel at the highest tested concentration (10  $\mu\text{M}$ ), displaying a wide selectivity window of at least more than two orders of magnitude between the antitrypanosomal activity ( $EC_{50}$  0.04  $\mu\text{M}$ ) and a potential inhibition of host's kinases. Since FS-554 (**2**), the compound which was taken as the starting point of the study, showed only a modest antitrypanosomal activity and selectivity in our test model ( $EC_{50}$  8.3  $\mu\text{M}$  and  $SI \sim 1$ ), we rate **3a** and four (**3b**, **3d**, **3f** and **3h**) of the most active and selective derivatives identified here ( $EC_{50} \leq 1 \mu\text{M}$  and  $SI \geq 60$ ) as substantial progress in our efforts to develop antitrypanosomal paullones. However, considering the wide difference between antitrypanosomal and TryS inhibitory activity, it is very improbable that TryS is the molecular target underlying the antiparasitic activity of **3a** and its congeners. Further studies are warranted to identify this target, e.g., by immobilizing compounds of series **3** on solid matrices and performing pull down assays with parasite cell homogenates.

Although some of the structures presented here exhibit potent antitrypanosomal activity and reasonable selectivity (e.g., **3a**, **3f**, **3h**), these are not looking very drug-like from a medicinal chemists point of view, displaying both high lipophilicity values and molecular masses. This impression is underlined by the very low solubility of the three mentioned compounds in aqueous phosphate buffer (Table 1). The optimization of the physicochemical parameters within this new antitrypanosomal compound family will therefore be a priority in further optimization studies.

#### 4. Conclusion

With a view to develop drugs against the unicellular parasite *T. brucei* and based on the observation that paullone FS-554 (**2**) is a potent or modest to weak inhibitor of TryS from the parasites *L. infantum* or *T. cruzi* and *T. brucei*, respectively, we have designed and synthesized 3-chlorokenpaullone derivatives with aryl instead of alkyl substitutions as potentially improved inhibitors of trypanosomatids TryS. This goal has, to some extent, been fulfilled for *Tc*TryS, with some of the novel paullones presenting a 3-fold higher activity than the lead structure scaffold. Although to an even minor level, most new derivatives also displayed a slightly improved inhibition of *Tb*TryS. In contrast, none of the new compounds could surpass the strong inhibition exerted by FS-554 (**2**) against TryS from *L. infantum*. Compared to the formerly investigated 9- and 11-substituted paullones the new series presented here represent an important advance in the generation of paullones with wider species-specificity for TryS. Nevertheless, the SAR analysis derived from testing paullones against TryS from three major trypanosomatid species provides strong evidence for the existence of peculiar demands for steric occupancy and polar interactions in the ATP-binding pocket of these enzymes. In this respect, future synthetic strategies of paullone analogues will address this subject by including novel alkyl substitutions at *N*(5) that may satisfy these demands. Not least, our data re-inforce the importance of testing

enzymes from different pathogens during screening campaigns aimed at detecting broad-range TryS inhibitors.

Importantly, several compounds showed potent antiparasitic activity and selectivity against the infective form of African trypanosomes. The wide difference between enzyme inhibitory concentration and antiparasitic activity casts doubt on TryS as responsible target. Because of its remarkable potent and selective antitrypanosomal activity together with its lack of inhibitory activity towards host kinases, structure **3a** ( $EC_{50}$  40 nM and  $SI > 1000$ ) can be rated as a promising new hit against African trypanosomiasis identified from this study. Thus, compound **3a** could serve as starting point for the development of derivatives with improved pharmacological properties. The identification of the responsible intracellular target underlying the antitrypanosomal activity of **3a** as well as its biological activity towards other pathogenic species of trypanosomatids will be of utmost importance for a rational drug development campaign in the future and therefore will be the subject of further studies, together with the optimization of physicochemical properties, namely the solubility in aqueous media.

#### 5. Experimental section

##### 5.1. Chemistry

###### 5.1.1. General

Melting points (mp) were determined on an electric variable heater (Barnstead Electrothermal IA 9100) in open glass capillaries and are not corrected. IR-spectra were recorded as KBr pellets on a Thermo Nicolet FT-IR 200.  $^1\text{H}$  NMR spectra and  $^{13}\text{C}$  NMR spectra were recorded on the following instruments: Bruker Avance DRX-400 and Bruker Avance II-600; solvent DMSO- $d_6$  if not stated otherwise; internal standard tetramethylsilane; signals in ppm ( $\delta$  scale). Elemental analyses were determined on a CE Instruments FlashEA<sup>®</sup> 1112 Elemental Analyser (Thermo Quest). Mass spectra were recorded on a double-focused sector field mass spectrometer Finnigan-MAT 90 or a MAT95XL (ThermoFinnigan MAT, Department of Mass Spectrometry of the Technische Universität Braunschweig). Accurate measurements were conducted according to the peakmatch method using perfluorokerosene (PFK) as an internal mass reference; (EI)-MS: ionization energy 70 eV. TLC: Polygram<sup>®</sup> Sil G/UV254, Macherey-Nagel, 40  $\times$  80 mm, visualization by UV-illumination (254 nm). Purity was determined by HPLC using the following devices and settings: Merck Hitachi LaChrom Elite system (DAD detector: L-2450 (isocrat.), UV detector: L-2400 (gradient); pump: L-2130; autosampler: L-2200; column: Merck LiChroCART 125-4, LiChrospher 100 RP-18 (5  $\mu\text{m}$ ); isocratic eluent: acetonitrile/water mixture; gradient elution (Method A): concentration acetonitrile 0–2 min: 10%; 2–12 min: 10%  $\rightarrow$  90% (linear) 12–20 min: 90%; gradient elution (Method B): concentration acetonitrile: 0–13 min: 10%  $\rightarrow$  90% (linear), 13–20 min: 90%; elution rate: 1.000 mL/min; detection wavelength: 254 nm and 280 nm (isocrat.), 254 nm (gradient); overall run time: 15 min (isocrat.);  $t_{\text{M}}$  = dead time related to DMSO;  $t_{\text{R}}$  = total retention time. All compounds employed in biological tests presented a purity >95%. Wavelength maxima were extracted from spectra generated by the DAD detector during HPLC analyses. Preparation of buffer for HPLC: To a mixture of trimethylamine (20.0 mL), sodium hydroxide (242 mg) and water (980 mL),  $\text{H}_2\text{SO}_4$  was added until the pH reached 2.7. THF was pre-dried over potassium hydroxide and subsequently distilled from  $\text{CaH}_2$ .  $\text{CH}_2\text{Cl}_2$  was dried by distillation from  $\text{CaH}_2$ . 4-Hydroxybenzylaminehydrobromide was prepared by refluxing 4-methoxybenzylamine with 5 equiv of 46% aqueous hydrobromic acid overnight, cooling to 0  $^\circ\text{C}$  and collecting the filtrate.<sup>42</sup> 3-Chlorokenpaullone **8** was synthesized according to a published method.<sup>41</sup> Other starting

materials were purchased from commercial suppliers (Acros Organics, Geel, Belgium; Sigma Aldrich, Steinheim, Germany) and were used without further purification.

### 5.1.2. *tert*-Butyl 2-(9-bromo-3-chloro-6-oxo-5,6,7,12-tetrahydrobenzo[2,3]azepino[4,5-*b*]indol-5-yl)acetate (9)

9-Bromo-3-chloro-7,12-dihydroindolo[3,2-*d*][1]benzazepin-6 (5*H*)-one (**8**, 610 mg, 1.68 mmol) was dissolved in dry THF (25 mL) under nitrogen. Potassium *tert*-butoxide (224 mg, 1.99 mmol) was added and the mixture stirred for 1 h at room temperature under nitrogen. After addition of *tert*-butyl 2-bromoacetate (390 mg, 1.99 mmol), dissolved in dry THF (50 mL), stirring was continued overnight at room temperature. Subsequently, the mixture was evaporated and the residue was dissolved in CH<sub>2</sub>Cl<sub>2</sub> (100 mL). The organic layer was washed with water (100 mL) and evaporated. The residue was crystallized from ethanol to yield a yellow powder (446 mg; 56%); mp: 278–281 °C; IR (KBr): 3333 cm<sup>-1</sup> (NH), 1736 cm<sup>-1</sup> (C=O), 1653 cm<sup>-1</sup> (C=O); <sup>1</sup>H NMR (400 MHz, *d*<sub>6</sub>-DMSO): δ (ppm) = 12.00 (s, 1H, indole-NH), 7.95 (d, 1H, *J* = 1.9 Hz, ArH), 7.74 (d, 1H, *J* = 8.4 Hz, ArH), 7.59 (d, 1H, *J* = 2.1 Hz, ArH), 7.50 (dd, 1H, *J* = 8.4, 2.1 Hz, ArH), 7.42 (d, 1H, *J* = 8.6 Hz, ArH), 7.30 (dd, 1H, *J* = 8.6, 1.9 Hz, ArH), 4.42 (s, 2H, *N*(5)-CH<sub>2</sub>), 3.97 and 3.09 (bs, 2H, azepine-CH<sub>2</sub>), 1.25 (s, 9H, *tert*-butyl); <sup>13</sup>C NMR (100.6 MHz, *d*<sub>6</sub>-DMSO): δ (ppm) = 27.4 (3C, *tert*-butyl); 30.9 (azepine-CH<sub>2</sub>), 52.7 (*N*(5)-CH<sub>2</sub>); 113.6, 120.7, 123.9, 124.9, 125.3, 128.7 (CH); 80.9, 109.2, 111.8, 124.3, 127.8, 132.5, 133.0, 136.0, 140.3, 168.1, 170.2 (C); CHN: calcd C 55.54, H 4.24, N 5.89, found C 55.93, H 4.33, N 5.59; C<sub>22</sub>H<sub>20</sub>BrClN<sub>2</sub>O<sub>3</sub> (475.76); MS (EI): *m/z* (%) = 476 ([M]<sup>+</sup>, 74), 420 ([M-56(-C<sub>4</sub>H<sub>8</sub>)]<sup>+</sup>, 100), 361 ([M-115(-C<sub>6</sub>H<sub>11</sub>O<sub>2</sub>)]<sup>+</sup>, 79); HPLC (isocrat.): 99.0% at 254 nm, 99.1% at 280 nm, *t*<sub>R</sub> = 3.96 min, *t*<sub>M</sub> (DMSO) = 1.07 min (ACN/H<sub>2</sub>O 50:50); λ<sub>max</sub>: 233 nm, 319 nm, 385 nm; HPLC (gradient): 95.2% at 254 nm, *t*<sub>R</sub> = 13.40 min, *t*<sub>M</sub> (DMSO) = 1.07 min (time: ACN/H<sub>2</sub>O; 0 min: 10/90; 10 min: 70/30; 10.5 min: 90/10; 22 min: 90/10).

### 5.1.3. 2-(9-Bromo-3-chloro-6-oxo-5,6,7,12-tetrahydrobenzo[2,3]azepino[4,5-*b*]indol-5-yl)acetic acid (10)

Trifluoroacetic acid (2 mL) was added to a suspension of *tert*-butyl 2-(9-bromo-3-chloro-6-oxo-5,6,7,12-tetrahydrobenzo[2,3]azepino[4,5-*b*]indol-5-yl)acetate (**9**, 296 mg, 0.622 mmol) in dry CH<sub>2</sub>Cl<sub>2</sub> (30 mL) under nitrogen. After stirring for 20 h at room temperature, the mixture was evaporated. Diethyl ether (3 mL) was added to the oily residue and the mixture was refluxed for 1 h. The resulting precipitate was filtered off, washed with diethyl ether and dried to yield a colorless powder (132 mg, 51%); mp: 207–208 °C (dec); IR (KBr): 3325 cm<sup>-1</sup> (NH), 1655 cm<sup>-1</sup> (C=O); <sup>1</sup>H NMR (400 MHz, *d*<sub>6</sub>-DMSO): δ (ppm) = 12.83 (bs, 1H, —OH), 12.01 (s, 1H, indole-NH), 7.96 (d, 1H, *J* = 1.9 Hz, ArH), 7.73 (d, 1H, *J* = 8.4 Hz, ArH), 7.58 (d, 1H, *J* = 2.0 Hz, ArH), 7.50 (dd, 1H, *J* = 8.4, 2.1 Hz, ArH), 7.42 (d, 1H, *J* = 8.6 Hz, ArH), 7.30 (dd, 1H, *J* = 8.6, 1.9 Hz, ArH), 4.39 (s, 2H, *N*(5)-CH<sub>2</sub>), 3.99 and 3.11 (bs, 2H, azepine-CH<sub>2</sub>); <sup>13</sup>C NMR (100.6 MHz, *d*<sub>6</sub>-DMSO): δ (ppm) = 31.0 (azepine-CH<sub>2</sub>), 52.3 (—*N*(5)-CH<sub>2</sub>); 113.6, 120.7, 123.7, 124.9, 125.3, 128.7 (CH<sub>2</sub>); 109.2, 111.9, 124.1, 127.8, 132.6, 133.0, 136.0, 140.6, 170.3, 170.7 (C); C<sub>18</sub>H<sub>12</sub>BrClN<sub>2</sub>O<sub>3</sub> (419.66); MS (EI): *m/z* (%) = 420 ([M]<sup>+</sup>, 100), 391 ([M-29(-CHO)]<sup>+</sup>, 40), 361 ([M-59(-C<sub>2</sub>H<sub>3</sub>O)]<sup>+</sup>, 61); HRMS (EI): *m/z* [M]<sup>+</sup> calcd 417.97143, found 417.97144; HPLC (isocrat.): 98.2% at 254 nm, 98.5% at 280 nm, *t*<sub>R</sub> = 3.99 min, *t*<sub>M</sub> (DMSO) = 1.07 min (ACN/H<sub>2</sub>O = 50:50); λ<sub>max</sub>: 234 nm, 318 nm, 398 nm.

### 5.1.4. General procedure for the preparation of *N*-substituted 2-(9-bromo-3-chloro-6-oxo-5,6,7,12-tetrahydrobenzo[2,3]azepino[4,5-*b*]indole-5-yl)acetamides 3a–3l

PyBOP and DIPEA were added to an ice-cooled solution of 2-(9-bromo-3-chloro-6-oxo-5,6,7,12-tetrahydrobenzo[2,3]azepino

[4,5-*b*]indol-5-yl)acetic acid (**10**) in DMF under nitrogen atmosphere. The solution was stirred at 0 °C for 20 min. The appropriate primary amine was added dropwise. The mixture was covered with a layer of argon and stirred for 20 h at room temperature. After addition of ethyl acetate (100 mL) the mixture was filtered and the collected precipitate was set aside. The organic solution was washed successively with 0.1 M aqueous hydrochloric acid (100 mL), 0.1 M aqueous sodium hydroxide solution (100 mL) and water (100 mL), then dried with Na<sub>2</sub>SO<sub>4</sub> and evaporated. The residue was combined with the precipitate collected by filtration and then crystallized from the indicated solvent.

**5.1.4.1. *N*-Benzyl-2-(9-bromo-3-chloro-6-oxo-5,6,7,12-tetrahydrobenzo[2,3]azepino[4,5-*b*]indole-5-yl)acetamide (3a).** Synthesized from 2-(9-bromo-3-chloro-6-oxo-5,6,7,12-tetrahydrobenzo[2,3]azepino[4,5-*b*]indol-5-yl)acetic acid (**10**, 202 mg, 481 μmol), DMF (1.0 mL), DIPEA (370 μL, 2.12 mmol), PyBOP (283 mg, 544 μmol) and benzylamine (65.4 μL, 601 μmol). The material was crystallized from tetrahydrofuran/toluene (1:1) to yield a colorless solid (128 mg, 53%); dec. starting at 337 °C; IR (KBr): 3316 cm<sup>-1</sup> (NH), 1663 cm<sup>-1</sup> (C=O); <sup>1</sup>H NMR (400 MHz, DMSO-*d*<sub>6</sub>): δ (ppm) = 11.99 (s, 1H, indole-NH), 8.66 (t, 1H, *J* = 6.0 Hz, NH), 7.97 (d, *J* = 2.0 Hz, 1H, ArH), 7.71 (m, 2H, ArH), 7.49 (dd, *J* = 8.4, 2.1 Hz, 1H, ArH), 7.44–7.40 (m, 1H, ArH), 7.36–7.21 (m, 6H, ArH), 4.35 (m, 4H, —*N*(5)-CH<sub>2</sub> and —CH<sub>2</sub>), 4.01 and 3.11 (bs, 2H, azepine-CH<sub>2</sub>); <sup>13</sup>C NMR (100.6 MHz, DMSO-*d*<sub>6</sub>): δ (ppm) = 31.2, 42.1, 53.5 (CH<sub>2</sub>); 113.6, 120.7, 124.1, 124.9, 125.1, 126.7, 127.0, (2C), 128.2 (2C), 128.6 (CH); 109.4, 111.8, 124.0, 127.8, 132.4, 133.0, 136.0, 139.2, 141.0, 168.3, 170.2 (C); CHN: calcd C 59.02, H 3.76; N 8.28, found C 58.86, H 3.74, N 8.75; C<sub>25</sub>H<sub>19</sub>BrClN<sub>3</sub>O<sub>2</sub> (508.79); MS (EI): *m/z* (%) = 509 [M]<sup>+</sup> (23), 402 [M-107(-C<sub>7</sub>H<sub>9</sub>N)]<sup>+</sup> (100); HRMS (EI): *m/z* [M]<sup>+</sup> calcd 507.03437, found 507.03409; HPLC (isocrat.): 96.9% at 254 nm, 96.2% at 280 nm, *t*<sub>R</sub> = 3.93 min, *t*<sub>M</sub> (DMSO) = 1.07 min (ACN/H<sub>2</sub>O = 60:40); λ<sub>max</sub>: 237 nm, 318 nm, 389 nm.

**5.1.4.2. 2-(9-Bromo-3-chloro-6-oxo-5,6,7,12-tetrahydrobenzo[2,3]azepino[4,5-*b*]indole-5-yl)-*N*-(4-chlorobenzyl)acetamide (3b).** Synthesized from 2-(9-bromo-3-chloro-6-oxo-5,6,7,12-tetrahydrobenzo[2,3]azepino[4,5-*b*]indol-5-yl)acetic acid (**10**, 293 mg, 698 μmol), DMF (1.4 mL), DIPEA (511 μL, 2.94 mmol), PyBOP (443 mg, 851 μmol) and 4-chlorobenzylamine (100 μL, 827 μmol). The material was crystallized twice from methanol to yield a colorless solid (114 mg, 30%); dec. starting at 305 °C; IR (KBr): 3316 cm<sup>-1</sup> (NH), 1639 cm<sup>-1</sup> (C=O), 1657 cm<sup>-1</sup> (C=O); <sup>1</sup>H NMR (600 MHz, DMSO-*d*<sub>6</sub>): δ (ppm) = 11.99 (s, 1H, indole-NH), 8.69 (t, *J* = 6.0 Hz, 1H, —NH), 7.97 (d, *J* = 1.9 Hz, 1H, ArH), 7.72 (d, *J* = 8.4 Hz, 1H, ArH), 7.67 (d, *J* = 2.1 Hz, 1H, ArH), 7.49 (dd, *J* = 8.4, 2.1 Hz, 1H, ArH), 7.42 (d, *J* = 8.6 Hz, 1H, ArH), 7.39–7.35 (m, 2H, ArH), 7.30 (dd, *J* = 8.6, 2.0 Hz, 1H, ArH), 7.29–7.26 (m, 2H, ArH), 4.31 (bs, 4H, —*N*(5)-CH<sub>2</sub> and —CH<sub>2</sub>), 3.99 and 3.12 (bs, 2H, azepine-CH<sub>2</sub>); <sup>13</sup>C NMR (151 MHz, DMSO-*d*<sub>6</sub>): δ (ppm) = 31.1, 41.4, 53.5 (CH<sub>2</sub>); 113.6, 120.7, 124.0, 124.8, 125.1, 128.1 (2C), 128.5, 128.8 (2C) (CH); 109.3, 111.8, 123.9, 127.7, 128.8, 131.2, 132.4, 135.9, 138.3, 140.9, 168.4, 170.2 (C); CHN: calcd C 55.27, H 3.34, N 7.74, found C 55.28, H 3.39, N 7.47; C<sub>25</sub>H<sub>18</sub>BrCl<sub>2</sub>N<sub>3</sub>O<sub>2</sub> (543.24); MS (EI): *m/z* (%) = 542.9 [M]<sup>+</sup> (24), 401.9 [M-141(-C<sub>7</sub>H<sub>7</sub>ClN)]<sup>+</sup> (100); HPLC (isocrat.): 99.2% at 254 nm, 99.5% at 280 nm, *t*<sub>R</sub> = 5.40 min, *t*<sub>M</sub> (DMSO) = 1.06 min (ACN/H<sub>2</sub>O = 60:40); λ<sub>max</sub>: 234 nm, 318 nm; HPLC (gradient method A): 98.5% at 254 nm, *t*<sub>R</sub> = 13.14 min.

**5.1.4.3. 2-(9-Bromo-3-chloro-6-oxo-5,6,7,12-tetrahydrobenzo[2,3]azepino[4,5-*b*]indole-5-yl)-*N*-(2-chlorobenzyl)acetamide (3c).** Synthesized from 2-(9-bromo-3-chloro-6-oxo-5,6,7,12-tetrahydrobenzo[2,3]azepino[4,5-*b*]indol-5-yl)acetic acid (**10**, 293 mg, 698 μmol), DMF (1.4 mL), DIPEA (511 μL, 2.94 mmol),

PyBOP (441 mg, 847  $\mu\text{mol}$ ) and 2-chlorobenzylamine (100  $\mu\text{L}$ , 827  $\mu\text{mol}$ ). The material was crystallized from methanol to yield a colorless solid (159 mg, 42%); dec. starting at 345  $^{\circ}\text{C}$ ; IR (KBr): 3422  $\text{cm}^{-1}$  (NH), 3312  $\text{cm}^{-1}$  (NH), 3262  $\text{cm}^{-1}$  (NH), 1654  $\text{cm}^{-1}$  (C=O);  $^1\text{H}$  NMR (600 MHz, DMSO- $d_6$ ):  $\delta$  (ppm) = 11.99 (s, 1H, indole-NH), 8.70 (t,  $J$  = 5.9 Hz, 1H, -NH), 7.97 (d,  $J$  = 1.9 Hz, 1H, ArH), 7.72 (d,  $J$  = 8.4 Hz, 1H, ArH), 7.69 (d,  $J$  = 2.1 Hz, 1H, ArH), 7.49 (dd,  $J$  = 8.4, 2.1 Hz, 1H, ArH), 7.47–7.43 (m, 1H, ArH), 7.42 (d,  $J$  = 8.6 Hz, 1H, ArH), 7.40–7.36 (m, 1H, ArH), 7.35–7.28 (m, 3H, ArH), 4.38 (bs, 4H, -N(5)-CH<sub>2</sub> and -CH<sub>2</sub>), 4.01 and 3.12 (bs, 2H, azepine-CH<sub>2</sub>);  $^{13}\text{C}$  NMR (151 MHz, DMSO- $d_6$ ):  $\delta$  (ppm) = 31.2, 40.1, 53.5 (CH<sub>2</sub>); 113.6, 120.8, 124.0, 124.9, 125.2, 127.1, 128.6 (3C), 129.1 (CH); 109.4, 111.9, 124.1, 127.8, 131.9, 132.5, 133.0, 136.0, 136.1, 141.0, 168.6, 170.33 (C); CHN: calcd C 55.27, H 3.34, N 7.74, found C 55.13, H 3.42, N 7.48; C<sub>25</sub>H<sub>18</sub>BrCl<sub>2</sub>N<sub>3</sub>O<sub>2</sub> (543.24); MS (EI):  $m/z$  (%): 543.0 [M]<sup>+</sup> (14), 401.9 [M-141(-C<sub>7</sub>H<sub>7</sub>ClN)]<sup>+</sup> (100); HPLC (isocrat.): 98.4% at 254 nm, 98.5% at 280 nm,  $t_{\text{R}}$  = 5.47 min,  $t_{\text{M}}$  (DMSO) = 1.06 min (ACN/H<sub>2</sub>O = 60:40);  $\lambda_{\text{max}}$ : 233 nm, 231 nm, 318 nm; HPLC (gradient method A): 98.3% at 254 nm,  $t_{\text{R}}$  = 13.01 min.

#### 5.1.4.4. 2-(9-Bromo-3-chloro-6-oxo-5,6,7,12-tetrahydrobenzo[2,3]azepino[4,5-*b*]indole-5-yl)-N-(3-chlorobenzyl)acetamide (3d).

Synthesized from 2-(9-bromo-3-chloro-6-oxo-5,6,7,12-tetrahydrobenzo[2,3]azepino[4,5-*b*]indol-5-yl)acetic acid (**10**, 294 mg, 700  $\mu\text{mol}$ ), DMF (1.4 mL), DIPEA (511  $\mu\text{L}$ , 2.94 mmol), PyBOP (442 mg, 849  $\mu\text{mol}$ ) and 3-chlorobenzylamine (100  $\mu\text{L}$ , 827  $\mu\text{mol}$ ). Crystallized from methanol yielded a colorless solid (95 mg, 25%); dec. starting at 342  $^{\circ}\text{C}$ ; IR (KBr): 3308  $\text{cm}^{-1}$  (NH), 1639  $\text{cm}^{-1}$  (C=O);  $^1\text{H}$  NMR (600 MHz, DMSO- $d_6$ ):  $\delta$  (ppm) = 11.99 (s, 1H, indole-NH), 8.73 (t,  $J$  = 6.0 Hz, 1H, NH), 7.98 (d,  $J$  = 1.9 Hz, 1H, ArH), 7.72 (d,  $J$  = 8.4 Hz, 1H, ArH), 7.67 (d,  $J$  = 2.1 Hz, 1H, ArH), 7.49 (dd,  $J$  = 8.4, 2.1 Hz, 1H, ArH), 7.42 (d,  $J$  = 8.6 Hz, 1H, ArH), 7.38–7.28 (m, 4H, ArH), 7.26–7.21 (m, 1H, ArH), 4.35 (bs, 4H, -N(5)-CH<sub>2</sub> and -CH<sub>2</sub>), 3.99 and 3.13 (bs, 2H, azepine-CH<sub>2</sub>);  $^{13}\text{C}$  NMR (151 MHz, DMSO- $d_6$ ):  $\delta$  (ppm) = 31.2, 41.6, 53.6 (CH<sub>2</sub>); 113.6, 120.8, 124.0, 124.1, 124.9, 125.2, 126.7, 126.9, 128.6, 130.1 (CH); 109.4, 111.9, 125.7, 127.8, 132.4, 133.0, 133.0, 136.0, 141.1, 141.9, 170.3, 168.6 (C); CHN: calcd C 55.27, H 3.34, N 7.74, found C 54.88, H 3.38, N 7.56; C<sub>25</sub>H<sub>18</sub>BrCl<sub>2</sub>N<sub>3</sub>O<sub>2</sub> (543.24); MS (EI):  $m/z$  (%): 542.9 [M]<sup>+</sup> (24), 401.9 [M-141(-C<sub>7</sub>H<sub>7</sub>ClN)]<sup>+</sup> (100); HPLC (isocrat.): 95.9% at 254 nm, 96.3% at 280 nm,  $t_{\text{R}}$  = 5.40 min,  $t_{\text{M}}$  (DMSO) = 1.06 min (ACN/H<sub>2</sub>O = 60:40);  $\lambda_{\text{max}}$ : 232 nm, 319 nm, 383 nm; HPLC (gradient method B): 96.7% at 254 nm,  $t_{\text{R}}$  = 13.38 min.

#### 5.1.4.5. 2-(9-Bromo-3-chloro-6-oxo-5,6,7,12-tetrahydrobenzo[2,3]azepino[4,5-*b*]indol-5-yl)-N-(3,4-dichlorobenzyl)acetamide (3e).

Synthesized from 2-(9-bromo-3-chloro-6-oxo-5,6,7,12-tetrahydrobenzo[2,3]azepino[4,5-*b*]indol-5-yl)acetic acid (**10**, 295 mg, 703  $\mu\text{mol}$ ), DMF (1.4 mL), DIPEA (511  $\mu\text{L}$ , 2.94 mmol), PyBOP (447 mg, 859  $\mu\text{mol}$ ) and 3,4-dichlorobenzylamine (100  $\mu\text{L}$ , 858  $\mu\text{mol}$ ). Crystallization from ethanol yielded a colorless solid (81 mg, 20%); mp: 325  $^{\circ}\text{C}$ ; IR (KBr): 3312  $\text{cm}^{-1}$  (NH), 1638  $\text{cm}^{-1}$  (C=O), 1654  $\text{cm}^{-1}$  (C=O);  $^1\text{H}$  NMR (600 MHz, DMSO- $d_6$ ):  $\delta$  (ppm) = 12.00 (s, 1H, indole-NH), 8.76 (t,  $J$  = 6.0 Hz, 1H, -NH), 7.98 (d,  $J$  = 1.9 Hz, 1H, ArH), 7.73 (d,  $J$  = 8.4 Hz, 1H, ArH), 7.66 (d,  $J$  = 2.1 Hz, 1H, ArH), 7.59 (d,  $J$  = 8.3 Hz, 1H, ArH), 7.54 (d,  $J$  = 2.0 Hz, 1H, ArH), 7.50 (dd,  $J$  = 8.4, 2.1 Hz, 1H, ArH), 7.43 (d,  $J$  = 8.4 Hz, 1H, ArH), 7.31 (dd,  $J$  = 8.6, 1.9 Hz, 1H, ArH), 7.27 (dd,  $J$  = 8.3, 2.0 Hz, 1H, ArH), 4.34 (bs, 4H, -N(5)-CH<sub>2</sub> and -CH<sub>2</sub>), 4.00 and 3.14 (bs, 2H, azepine-CH<sub>2</sub>);  $^{13}\text{C}$  NMR (151 MHz, DMSO- $d_6$ ):  $\delta$  (ppm) = 31.2, 41.1, 53.7 (CH<sub>2</sub>); 113.7, 120.8, 124.1, 124.9, 125.2, 127.4, 128.6, 129.0, 130.4 (CH); 109.4, 111.9, 124.0, 127.8, 129.3, 131.0, 132.5, 133.0, 136.0, 140.6, 141.0, 168.7, 170.4 (C); CHN: calcd C 51.98, H 2.97, N 7.27, found C 52.13, H 2.79, N 7.07; C<sub>25</sub>H<sub>17</sub>BrCl<sub>3</sub>N<sub>3</sub>O<sub>2</sub> (577.68); MS (EI):  $m/z$  (%): 576.9 [M]<sup>+</sup> (24),

402.0 [M-174.9(-C<sub>7</sub>H<sub>6</sub>Cl<sub>2</sub>N)]<sup>+</sup> (100); HPLC (isocrat.) 99.5% at 254 nm, 99.6% at 280 nm,  $t_{\text{R}}$  = 7.5 min,  $t_{\text{M}}$  (DMSO) = 1.06 min (ACN/H<sub>2</sub>O = 60:40);  $\lambda_{\text{max}}$ : 228 nm, 319 nm; HPLC (gradient method A): 99.7% at 254 nm,  $t_{\text{R}}$  = 13.6 min.

#### 5.1.4.6. 2-(9-Bromo-3-chloro-6-oxo-5,6,7,12-tetrahydrobenzo[2,3]azepino[4,5-*b*]indol-5-yl)-N-(4-methylbenzyl)acetamide (3f).

Synthesized from 2-(9-bromo-3-chloro-6-oxo-5,6,7,12-tetrahydrobenzo[2,3]azepino[4,5-*b*]indol-5-yl)acetic acid (**10**, 296 mg, 705  $\mu\text{mol}$ ), DMF (1.4 mL), DIPEA (511  $\mu\text{L}$ , 2.94 mmol), PyBOP (440 mg, 846  $\mu\text{mol}$ ) and 4-methylbenzylamine (100  $\mu\text{L}$ , 786  $\mu\text{mol}$ ). Crystallization from methanol yielded a colorless solid (120 mg, 33%); dec. starting at 326  $^{\circ}\text{C}$ ; IR (KBr): 3317  $\text{cm}^{-1}$  (NH), 1653  $\text{cm}^{-1}$  (C=O), 1640  $\text{cm}^{-1}$  (C=O);  $^1\text{H}$  NMR (600 MHz, DMSO- $d_6$ ):  $\delta$  (ppm) = 11.99 (s, 1H, indole-NH), 8.60 (t,  $J$  = 6.0 Hz, 1H, -NH), 7.97 (d,  $J$  = 1.9 Hz, 1H, ArH), 7.72 (d,  $J$  = 8.4 Hz, 1H, ArH), 7.68 (d,  $J$  = 2.1 Hz, 1H, ArH), 7.49 (dd,  $J$  = 8.4, 2.1 Hz, 1H, ArH), 7.42 (d,  $J$  = 8.6 Hz, 1H, ArH), 7.30 (dd,  $J$  = 8.6, 1.9 Hz, 1H, ArH), 7.13 (q,  $J$  = 8.0 Hz, 4H, ArH), 4.28 (bs, 4H, -N(5)-CH<sub>2</sub> and -CH<sub>2</sub>), 3.99 and 3.11 (bs, 2H, azepine-CH<sub>2</sub>), 2.28 (s, 3H, -CH<sub>3</sub>);  $^{13}\text{C}$  NMR (151 MHz, DMSO- $d_6$ ):  $\delta$  (ppm) = 20.7 (CH<sub>3</sub>); 31.2, 41.9, 53.5 (CH<sub>2</sub>); 113.6, 120.8, 124.1, 124.9, 125.2, 127.0 (2C), 128.6, 128.8 (2C) (CH); 109.4, 111.9, 124.0, 127.8, 132.5, 133.0, 135.8, 136.0, 136.2, 141.1, 168.2, 170.2 (C); CHN: calcd C 59.73, H 4.05, N 8.04, found C 59.70, H 4.03, N 7.81; C<sub>26</sub>H<sub>21</sub>BrClN<sub>3</sub>O<sub>2</sub> (522.83); MS (EI):  $m/z$  (%): 523.0 [M]<sup>+</sup> (24), 402.0 [M-121(-C<sub>8</sub>H<sub>11</sub>N)]<sup>+</sup> (100); HPLC (isocrat.): 99.2% at 254 nm, 99.2% at 280 nm,  $t_{\text{R}}$  = 5.37 min,  $t_{\text{M}}$  (DMSO) = 1.06 min (ACN/H<sub>2</sub>O = 60:40);  $\lambda_{\text{max}}$ : 236 nm, 318 nm, 391 nm; HPLC (gradient method B): 99.1% at 254 nm,  $t_{\text{R}}$  = 13.21 min.

#### 5.1.4.7. 2-(9-Bromo-3-chloro-6-oxo-5,6,7,12-tetrahydrobenzo[2,3]azepino[4,5-*b*]indol-5-yl)-N-(4-methoxybenzyl)acetamide (3g).

Synthesized from 2-(9-bromo-3-chloro-6-oxo-5,6,7,12-tetrahydrobenzo[2,3]azepino[4,5-*b*]indol-5-yl)acetic acid (**10**, 217 mg, 517  $\mu\text{mol}$ ), DMF (1.0 mL), DIPEA (370  $\mu\text{L}$ , 2.12 mmol), PyBOP (318 mg, 611  $\mu\text{mol}$ ) and 4-methoxybenzylamine (83  $\mu\text{L}$ , 635  $\mu\text{mol}$ ). Crystallization from methanol yielded a colorless solid (82 mg, 29%); dec. starting at 313  $^{\circ}\text{C}$ ; IR (KBr): 3314  $\text{cm}^{-1}$  (NH), 1654  $\text{cm}^{-1}$  (C=O), 1640  $\text{cm}^{-1}$  (C=O);  $^1\text{H}$  NMR (600 MHz, DMSO- $d_6$ ):  $\delta$  (ppm) = 12.00 (s, 1H, indole-NH), 8.59 (t,  $J$  = 5.9 Hz, 1H, -NH), 7.98 (d,  $J$  = 1.9 Hz, 1H, ArH), 7.73 (d,  $J$  = 8.4 Hz, 1H, ArH), 7.69 (d,  $J$  = 2.1 Hz, 1H, ArH), 7.50 (dd,  $J$  = 8.4, 2.1 Hz, 1H, ArH), 7.43 (d,  $J$  = 8.6 Hz, 1H, ArH), 7.31 (dd,  $J$  = 8.6, 1.9 Hz, 1H, ArH), 7.23–7.16 (m, 2H, ArH), 6.94–6.85 (m, 2H, ArH), 4.26 (bs, 4H, -N(5)-CH<sub>2</sub> and -CH<sub>2</sub>), 4.00 and 3.13 (bs, 2H, azepine-CH<sub>2</sub>), 3.75 (s, 3H, -OCH<sub>3</sub>);  $^{13}\text{C}$  NMR (151 MHz, DMSO- $d_6$ ):  $\delta$  (ppm) = 54.8 (CH<sub>3</sub>); 30.9, 41.4, 53.3 (CH<sub>2</sub>); 113.4 (2C), 120.5, 123.9, 124.7, 124.9, 128.2 (2C), 128.4 (CH); 109.4, 111.9, 124.0, 127.8, 131.1, 132.5, 133.0, 136.0, 141.1, 158.2, 168.2, 170.2 (C); CHN: calcd C 57.96, H 3.93, N 7.80, found C 57.76, H 3.74, N 7.45; C<sub>26</sub>H<sub>21</sub>BrClN<sub>3</sub>O<sub>3</sub> (538.83); MS (EI):  $m/z$  (%): 539.0 [M]<sup>+</sup> (24), 402.0 [M-137(-C<sub>8</sub>H<sub>11</sub>NO)]<sup>+</sup> (100); HPLC (isocrat.): 99.1% at 254 nm, 99.4% at 280 nm,  $t_{\text{R}}$  = 5.37 min,  $t_{\text{M}}$  (DMSO) = 1.06 min (ACN/H<sub>2</sub>O = 60:40);  $\lambda_{\text{max}}$ : 235 nm, 318 nm, 389 nm; HPLC (gradient method B): 99.6% at 254 nm,  $t_{\text{R}}$  = 12.45 min.

#### 5.1.4.8. 2-(9-Bromo-3-chloro-6-oxo-5,6,7,12-tetrahydrobenzo[2,3]azepino[4,5-*b*]indol-5-yl)-N-(4-hydroxybenzyl)acetamide (3h).

Synthesized from 2-(9-bromo-3-chloro-6-oxo-5,6,7,12-tetrahydrobenzo[2,3]azepino[4,5-*b*]indol-5-yl)acetic acid (**10**, 295 mg, 703  $\mu\text{mol}$ ), DMF (1.4 mL), DIPEA (1.02 mL, 5.88 mmol), PyBOP (449 mg, 862  $\mu\text{mol}$ ) and 4-hydroxybenzylaminehydrobromide (178 mg, 873  $\mu\text{mol}$ ). Crystallization from ethanol yielded a colorless solid (146 mg, 40%); dec. starting at 280  $^{\circ}\text{C}$ ; IR (KBr): 3312  $\text{cm}^{-1}$  (NH), 1638  $\text{cm}^{-1}$  (C=O), 1654  $\text{cm}^{-1}$  (C=O);  $^1\text{H}$  NMR

(600 MHz, DMSO-*d*<sub>6</sub>):  $\delta$  (ppm) = 12.00 (s, 1H, indole-NH), 9.31 (s, 1H, –OH), 8.54 (t, *J* = 5.9 Hz, 1H, –NH), 7.98 (d, *J* = 1.9 Hz, 1H, ArH), 7.73 (d, *J* = 8.4 Hz, 1H, ArH), 7.68 (d, *J* = 2.1 Hz, 1H, ArH), 7.49 (dd, *J* = 8.4, 2.1 Hz, 1H, ArH), 7.43 (d, *J* = 8.6 Hz, 1H, ArH), 7.10–7.05 (m, 2H, ArH), 7.31 (dd, *J* = 8.6, 2.0 Hz, 1H, ArH), 6.79–6.65 (m, 2H, ArH), 4.22 (s, 4H, –N(5)–CH<sub>2</sub> and –CH<sub>2</sub>), 4.01 and 3.13 (s, 2H, azepine-CH<sub>2</sub>); <sup>13</sup>C NMR (151 MHz, DMSO-*d*<sub>6</sub>):  $\delta$  (ppm) = 31.2, 41.7, 53.5 (CH<sub>2</sub>); 113.7, 115.0 (2C), 120.8, 124.1, 124.9, 125.2, 128.4 (2C), 128.6 (CH); 109.4, 111.9, 124.0, 127.8, 129.3, 132.5, 133.0, 136.0, 141.1, 156.3, 168.1, 170.2 (C); CHN: calcd C 57.22, H 3.65, N 8.01, found C 56.88, H 3.85, N 7.74; C<sub>25</sub>H<sub>19</sub>BrClN<sub>3</sub>O<sub>3</sub> (524.80); MS (EI): *m/z* (%): 525.0 [M]<sup>+</sup> (21), 402.0 [M–123(–C<sub>7</sub>H<sub>9</sub>NO)]<sup>+</sup> (100); HPLC (isocrat.): 98.3% at 254 nm, 99.0% at 280 nm, *t*<sub>R</sub> = 4.50 min, *t*<sub>M</sub> (DMSO) = 1.06 min (ACN/H<sub>2</sub>O = 50:50);  $\lambda_{\text{max}}$ : 228 nm, 319 nm, 390 nm; HPLC (gradient method A): 95.5% at 254 nm, *t*<sub>R</sub> = 11.3 min.

#### 5.1.4.9. 2-(9-Bromo-3-chloro-6-oxo-5,6,7,12-tetrahydrobenzo[2,3]azepino[4,5-*b*]indol-5-yl)-N-(4-(trifluoromethyl)benzyl)acetamide (3i).

Synthesized from 2-(9-bromo-3-chloro-6-oxo-5,6,7,12-tetrahydrobenzo[2,3]azepino[4,5-*b*]indol-5-yl)acetic acid (210 mg, 500  $\mu$ mol), DMF (1.0 mL), DIPEA (370  $\mu$ L, 2.12 mmol), PyBOP (316 mg, 607  $\mu$ mol) and 4-trifluoromethylbenzylamine (88  $\mu$ L, 615  $\mu$ mol). Crystallization from ethanol yielded a colorless solid (43 mg, 15%); dec. starting at 321 °C; IR (KBr): 3312 cm<sup>–1</sup> (NH), 1639 cm<sup>–1</sup> (C=O), 1659 cm<sup>–1</sup> (C=O); <sup>1</sup>H NMR (600 MHz, DMSO-*d*<sub>6</sub>):  $\delta$  (ppm) = 12.01 (s, 1H, indole-NH), 8.79 (t, *J* = 6.0 Hz, 1H, –NH), 7.98 (d, *J* = 2.0 Hz, 1H, ArH), 7.73 (d, *J* = 8.4 Hz, 1H, ArH), 7.71–7.66 (m, 3H, ArH), 7.51–7.49 (m, 3H, ArH), 7.45–7.42 (m, 1H, ArH), 7.31 (dd, *J* = 8.6, 2.0 Hz, 1H, ArH), 4.43 (bs, 4H, –N(5)–CH<sub>2</sub> and –CH<sub>2</sub>), 4.01 and 3.14 (bs, 2H, azepine-CH<sub>2</sub>); <sup>13</sup>C NMR (151 MHz, DMSO-*d*<sub>6</sub>):  $\delta$  (ppm) = 31.2, 41.8, 53.6 (CH<sub>2</sub>); 113.4, 120.5, 123.9, 124.7, 124.9 (2C, q, *J* = 3.8 Hz), 125.0, 127.5 (2C), 128.4 (CH); 109.4, 111.9, 124.0, 124.4 (q, *J* = 271.8 Hz), 127.5 (q, *J* = 31.6 Hz), 132.5, 133.0, 136.0, 141.0, 144.3, 168.6, 170.3 (C); CHN: calcd C 54.14, H 3.15, N 7.29, found C 53.97, H 3.01, N 6.95; C<sub>26</sub>H<sub>18</sub>BrClF<sub>3</sub>N<sub>3</sub>O<sub>2</sub> (576.80); MS (EI): *m/z* (%): 577.0 [M]<sup>+</sup> (28), 402.0 [M–175(–C<sub>8</sub>H<sub>8</sub>F<sub>3</sub>N)]<sup>+</sup> (100); HPLC (isocrat.): 98.5% at 254 nm, 98.8% at 280 nm, *t*<sub>R</sub> = 6.51 min, *t*<sub>M</sub> (DMSO) = 1.06 min (ACN/H<sub>2</sub>O = 60:40);  $\lambda_{\text{max}}$ : 228 nm, 319 nm, 390 nm; HPLC (gradient method B): 98.0% at 254 nm, *t*<sub>R</sub> = 13.2 min.

#### 5.1.4.10. 2-(9-Bromo-3-chloro-6-oxo-5,6,7,12-tetrahydrobenzo[2,3]azepino[4,5-*b*]indol-5-yl)-N-(pyridin-4-ylmethyl)acetamide (3j).

Synthesized from 2-(9-bromo-3-chloro-6-oxo-5,6,7,12-tetrahydrobenzo[2,3]azepino[4,5-*b*]indol-5-yl)acetic acid (10, 211 mg, 503  $\mu$ mol), DMF (1.0 mL), DIPEA (370  $\mu$ L, 2.12 mmol), PyBOP (280 mg, 538  $\mu$ mol) and 4-pyridinemethanamine (61  $\mu$ L, 601  $\mu$ mol). Crystallization from methanol yielded a colorless solid (83 mg, 33%); dec. starting at 301 °C; IR (KBr): 3401 cm<sup>–1</sup> (NH), 3231 cm<sup>–1</sup> (NH), 1654 cm<sup>–1</sup> (C=O), 1687 cm<sup>–1</sup> (C=O); <sup>1</sup>H NMR (600 MHz, DMSO-*d*<sub>6</sub>):  $\delta$  (ppm) = 12.00 (s, 1H, indole-NH), 8.78 (t, *J* = 6.0 Hz, 1H, –NH), 8.55–8.45 (m, 2H, ArH), 7.98 (d, *J* = 1.9 Hz, 1H, ArH), 7.73 (d, *J* = 8.4 Hz, 1H, ArH), 7.69 (d, *J* = 2.1 Hz, 1H, ArH), 7.50 (dd, *J* = 8.4, 2.1 Hz, 1H, ArH), 7.42 (d, *J* = 8.6 Hz, 1H, ArH), 7.30 (dd, *J* = 8.6, 1.9 Hz, 1H, ArH), 7.28–7.25 (m, 2H, ArH), 4.36 (bs, 4H, –N(5)–CH<sub>2</sub> and –CH<sub>2</sub>), 4.01 and 3.13 (bs, 2H, azepine-CH<sub>2</sub>); <sup>13</sup>C NMR (151 MHz, DMSO-*d*<sub>6</sub>):  $\delta$  (ppm) = 31.2, 41.2, 53.6 (CH<sub>2</sub>); 113.6, 120.8, 121.9 (2C), 124.2, 124.9, 125.2, 128.6, 149.4 (2C) (CH); 148.4, 109.4, 111.9, 124.0, 127.8, 132.5, 133.0, 136.0, 141.0, 168.8, 170.4 (C); CHN: calcd C 56.55, H 3.56, N 10.99, found C 56.31, H 3.54, N 10.60; C<sub>24</sub>H<sub>18</sub>BrClN<sub>4</sub>O<sub>2</sub> (509.79); MS (EI): *m/z* (%): 510.0 [M]<sup>+</sup> (24), 402.0 [M–108.0(–C<sub>6</sub>H<sub>8</sub>N<sub>2</sub>)]<sup>+</sup> (100); HPLC (isocrat.): 97.7% at 254 nm, 98.2% at 280 nm, *t*<sub>R</sub> = 4.79 min, *t*<sub>M</sub> (DMSO) = 1.06 min (ACN/Buffer = 40:60);  $\lambda_{\text{max}}$ : 232 nm, 319 nm.

#### 5.1.4.11. 2-(9-Bromo-3-chloro-6-oxo-5,6,7,12-tetrahydrobenzo[2,3]azepino[4,5-*b*]indol-5-yl)-N-(pyridin-3-ylmethyl)acetamide (3k).

Synthesized from 2-(9-bromo-3-chloro-6-oxo-5,6,7,12-tetrahydrobenzo[2,3]azepino[4,5-*b*]indol-5-yl)acetic acid (10, 218 mg, 519  $\mu$ mol), DMF (1.0 mL), DIPEA (370  $\mu$ L, 2.12 mmol), PyBOP (340 mg, 653  $\mu$ mol), and 3-pyridinemethanamine (61  $\mu$ L, 599  $\mu$ mol). Crystallization from methanol yielded a colorless solid (38 mg, 14%); dec. starting at 308 °C; IR (KBr): 3348 cm<sup>–1</sup> (NH), 1698 cm<sup>–1</sup> (C=O), 1645 cm<sup>–1</sup> (C=O); <sup>1</sup>H NMR (600 MHz, DMSO-*d*<sub>6</sub>):  $\delta$  (ppm) = 12.00 (s, 1H, indole-NH), 8.79 (t, *J* = 6.0 Hz, 1H, –NH), 8.54–8.52 (m, 1H, ArH), 7.98 (d, *J* = 1.9 Hz, 1H, ArH), 7.78 (dd, *J* = 7.7, 1.8 Hz, 1H, ArH), 7.76–7.72 (m, 2H, ArH), 7.51 (dd, *J* = 8.4, 2.1 Hz, 1H, ArH), 7.43 (d, *J* = 8.6 Hz, 1H, ArH), 7.36–7.23 (m, 3H, ArH), 4.34 (bs, 4H, –N(5)–CH<sub>2</sub> and –CH<sub>2</sub>), 4.01 and 3.15 (bs, 2H, azepine-CH<sub>2</sub>); <sup>13</sup>C NMR (151 MHz, DMSO-*d*<sub>6</sub>):  $\delta$  (ppm) = 31.0, 43.9, 53.5 (CH<sub>2</sub>); 113.4, 120.5, 120.6, 121.8, 123.9, 124.7, 125.0, 128.4, 136.4, 148.6 (CH); 109.4, 111.9, 124.0, 127.8, 132.5, 133.0, 136.0, 141.1, 158.4, 168.6, 170.3 (C); CHN: calcd C 56.55, H 3.56, N 10.99, found C 56.47, H 3.80, N 10.65; C<sub>24</sub>H<sub>18</sub>BrClN<sub>4</sub>O<sub>2</sub> (509.79); MS (EI): *m/z* (%): 510.0 [M]<sup>+</sup> (49), 402.0 [M–108.0(–C<sub>6</sub>H<sub>8</sub>N<sub>2</sub>)]<sup>+</sup> (100); HPLC (isocrat.): 99.6% at 254 nm, 99.6% at 280 nm, *t*<sub>R</sub> = 3.40 min, *t*<sub>M</sub> (DMSO) = 1.06 min (ACN/Buffer = 40:60);  $\lambda_{\text{max}}$ : 232 nm, 319 nm.

#### 5.1.4.12. 2-(9-Bromo-3-chloro-6-oxo-5,6,7,12-tetrahydrobenzo[2,3]azepino[4,5-*b*]indol-5-yl)-N-(pyridin-2-ylmethyl)acetamide (3l).

Synthesized from 2-(9-bromo-3-chloro-6-oxo-5,6,7,12-tetrahydrobenzo[2,3]azepino[4,5-*b*]indol-5-yl)acetic acid (10, 218 mg, 519  $\mu$ mol), DMF (1.0 mL), DIPEA (370  $\mu$ L, 2.12 mmol), PyBOP (284 mg, 546  $\mu$ mol), and 2-pyridinemethanamine (61  $\mu$ L, 623  $\mu$ mol). Crystallization from methanol yielded a colorless solid (26 mg, 10%); dec. starting at 313 °C; IR (KBr): 3300 cm<sup>–1</sup> (NH), 1643 cm<sup>–1</sup> (C=O); <sup>1</sup>H NMR (600 MHz, DMSO-*d*<sub>6</sub>):  $\delta$  (ppm) = 12.01 (s, 1H, indole-NH), 8.79 (t, *J* = 6.1 Hz, 1H, –NH), 8.60–8.39 (m, 2H, ArH), 7.99 (d, *J* = 1.9 Hz, 1H, ArH), 7.74 (d, *J* = 8.4 Hz, 1H, ArH), 7.70 (d, *J* = 2.1 Hz, 1H, ArH), 7.51 (dd, *J* = 8.4, 2.1 Hz, 1H, ArH), 7.43 (d, *J* = 8.5 Hz, 1H, ArH), 7.31 (dd, *J* = 8.6, 2.0 Hz, 1H, ArH), 7.29–7.26 (m, 2H, ArH), 4.37 (bs, 4H, –N(5)–CH<sub>2</sub> and –CH<sub>2</sub>), 4.02 and 3.14 (bs, 2H, azepine-CH<sub>2</sub>); <sup>13</sup>C NMR (151 MHz, DMSO-*d*<sub>6</sub>):  $\delta$  (ppm) = 30.9, 40.9, 53.4 (CH<sub>2</sub>); 113.4, 120.5, 121.7 (2C), 123.91, 124.7, 125.0, 128.4, 149.2 (2C) (CH); 109.4, 111.9, 124.1, 127.8, 132.5, 133.0, 136.0, 141.0, 148.4, 168.8, 170.4 (C); CHN: calcd C 56.55, H 3.56, N 10.99, found C 55.95, H 3.42, N 10.43; C<sub>24</sub>H<sub>18</sub>BrClN<sub>4</sub>O<sub>2</sub> (509.79); MS (EI): *m/z* (%): 510.0 [M]<sup>+</sup> (13), 402.0 [M–108.0(–C<sub>6</sub>H<sub>8</sub>N<sub>2</sub>)]<sup>+</sup> (100); HRMS (EI): *m/z* [M]<sup>+</sup>: calcd 508.02962, found 508.03027; HPLC (isocrat.): 99.5% at 254 nm, 99.9% at 280 nm, *t*<sub>R</sub> = 3.75 min, *t*<sub>M</sub> (DMSO) = 1.06 min (ACN/Buffer = 50:50);  $\lambda_{\text{max}}$ : 232 nm, 319 nm, 389 nm.

## 5.2. Biochemical and biological assays

### 5.2.1. Expression, purification and activity assay of trypanothione synthetase (TryS)

**5.2.1.1. Expression and purification of recombinant TryS.** The recombinant expression and purification of His-tagged TryS from *T. brucei*, *T. cruzi* and *L. infantum* was conducted as essentially described in Maiwald et al.<sup>34</sup>, and Sousa et al.<sup>19</sup> The expression vectors for *TbTryS*, *LiTryS* and *TcTryS* were kindly provided by Dr. Alan Fairlamb (Dundee University, UK), Dr. Ana Tomás (IBMC, Portugal) and Dr. Sergio Guerrero (Universidad Nacional del Litoral, Argentina). All recombinant proteins were expressed using *Escherichia coli* strain BL21(DE3) as host and Terri-fic Broth or auto-induction medium devoid of trace elements. For the first growth medium, 0.5 mM isopropyl 1-thio- $\beta$ -D-galactopyranoside were added to induce recombinant protein expression

during 5 h at 25 °C. In the autoinduction medium, cells were grown at 37 °C for 5 h and then at 25 °C for further 16–18 h. After physical (sonication) and enzymatic (lysozyme) cell lysis, the clarified supernatant was applied to a Ni-NTA resin and the recombinant TryS further purified to homogeneity by gel filtration and/or ion-exchange chromatography at room temperature and using an Äkta-FPLC device (GE Healthcare). Protein purity (for all TryS  $\geq 95\%$ ) was assessed after each purification step by SDS-PAGE 12% gel under reducing conditions. Protein concentration was determined by the Bicinchoninic Acid assay with bovine serum albumin as standard and enzyme activity was determined by the end-point assay detailed below (see 'TryS activity assay'). The purified proteins were stored at  $-20\text{ °C}$  in reaction buffer added of 40% (v/v) glycerol (Carlo Erba Reagents SA) without significant loss of activity for at least 6 months.

**5.2.1.2. TryS activity assay.** The end-point assay is based on the determination of inorganic phosphate released from ATP during TryS catalysis, by its complexation (phosphomolybdate) to the cationic triphenylmethane dye, malachite green (BIOMOL GREEN™ Enzo® Life Sciences). The green complex presents an absorption maximum at 650 nm. For all TryS, ATP was used at 150  $\mu\text{M}$  because of high background signal at higher concentrations and spermidine fixed at 2 mM, a concentration that resembles the intracellular levels calculated from data reported in the literature for different trypanosomatids<sup>43–45</sup>. Glutathione was adjusted to 0.05, 0.57 and 0.25 mM for *TbTryS*, *TcTryS* and *LiTryS*, respectively, concentrations that avoid substrate inhibition or correspond with reported intracellular contents.<sup>46</sup>

A master mix (MM) solution containing all the substrates at 1.25-fold their end concentration in assay was prepared in reaction buffer (5 mM DTT, 10 mM  $\text{MgSO}_4$ , 0.5 mM EDTA, 100 mM HEPES pH 7.4, 9 mM NaCl, 10% v/v DMSO) and kept on ice until use. Microtiter plate wells were loaded with 5  $\mu\text{L}$  of test compound, DMSO (reaction control) or TryS-specific inhibitor (inhibition control) and 40  $\mu\text{L}$  of MM. The reactions were then started by adding 5  $\mu\text{L}$  of TryS (1, 2 and 3  $\times 10^{-5}$   $\mu\text{mol min}^{-1} \text{mL}^{-1}$  for *TcTryS*, *LiTryS* and *TbTryS*, respectively) and stopped after 15 min with 200  $\mu\text{L}$  BIOMOL GREEN™ reagent. Blanks were prepared for each condition by adding 5  $\mu\text{L}$  of reaction buffer with 150 mM NaCl instead of enzyme.

The TryS activity is calculated as follow: % TryS activity =  $\frac{\{(A_{650 \text{ nm Ci}} - A_{650 \text{ nm Cib}}) / (A_{650 \text{ nm E}} - A_{650 \text{ nm EB}})\} \times 100}$ , where  $A_{650 \text{ nm Ci}}$  is the mean absorbance at 650 nm for the reaction test with compound i,  $A_{650 \text{ nm Cib}}$  is the mean absorbance at 650 nm for the blank control with compound i,  $A_{650 \text{ nm E}}$  is the mean absorbance at 650 nm for the reaction control with DMSO and  $A_{650 \text{ nm EB}}$  is the mean absorbance at 650 nm for the blank control with DMSO. The assays yielded an intra-assay coefficient variation ( $CV = \sigma^{n-1}_E/E$ )  $\leq 2.5\%$ , a signal to background coefficient ( $E/E_B$ ) of  $\sim 3.5$  and a Z' factor  $\geq 0.85$ .

### 5.2.2. Proliferation assay for infective *T. brucei brucei*

The biological activity of the compounds was evaluated in the infective form of *T. brucei brucei* strain 427, cell line 449 (encoding one copy of the tet-repressor protein: Pleo)<sup>47</sup> transfected with a construct encoding a redox biosensor (Sardi, Comini unpublished). The cultivation of the parasites and the viability assay were performed as previously described by Maiwald et al.<sup>34</sup> Stock solutions at 3–24 mM in DMSO were prepared for each compound according to their solubility. All compounds were subjected to a primary screening at 5 and 30  $\mu\text{M}$ . For compounds showing more than 90% parasite growth inhibition at 5  $\mu\text{M}$ ,  $\text{EC}_{50}$  values were determined. To determine  $\text{EC}_{50}$ , twofold serial dilutions in DMSO were prepared from the compound's stock solution. Two hundred microliter of trypanosomes in mid-exponential phase ( $\sim 2$  million cells/mL) were seeded in a 96-well culture plate (Corning Incorporated,

costar® 3599) at a cell density of  $5 \times 10^5$  cells/mL and treated with 2  $\mu\text{L}$  compound or DMSO (proliferation control). After 24 h, 100  $\mu\text{L}$  from each well was transferred to individual 1.1 mL tubes (T100, Biotube™ System), diluted with 200  $\mu\text{L}$  sterile phosphate buffered saline, pH 7.0, with 1% (w/v) glucose and added of 2  $\mu\text{L}$  propidium iodide (exclusion dye) at 200  $\mu\text{g/mL}$ , homogenized by quick vortexing and analyzed using a CyAn™ ADP (DakoCytomation) flow cytometer. Flow cytometry analysis was performed with a 488 nm solid-state laser as the excitation light source. The positive events (cells) were gated by forward-scatter (FSC) and side-scatter (SSC) parameters whereas the fluorescence of propidium iodide was collected at  $\lambda_{\text{em}} = 613/30 \text{ nm}$  to distinguish dead cells. The signals were detected with logarithmic amplifiers. All measurements were made at constant flow and acquisition time (60 s per sample). The data were analyzed using the Summit (Dako) and Flow-Jo (Tree star Inc.) software. A positive control included Nifurtimox (Lampit® from Bayer) tested at its  $\text{EC}_{50}$  (15  $\mu\text{M}$ ). All conditions were tested by triplicate.

The relative percentage of viable parasites at 5 or 30  $\mu\text{M}$  is expressed as follow:

$$\% \text{viability} = \left[ \frac{\text{(number of parasites for compound X at concentration Y)}}{\text{(number of parasites in the proliferation control)}} \right] \times 100.$$

The  $\text{EC}_{50}$  values were obtained from dose response curves fitted to a sigmoidal Boltzmann equation (errors calculated using errors' propagation) or extrapolated from non-linear fitting plots. The error is expressed as 2 S.D., estimated as  $2\sigma^{n-1}$ .

### 5.2.3. Cytotoxicity in murine macrophages

The J774 mouse macrophage cell line was cultivated in a humidified 5%  $\text{CO}_2/95\%$  air atmosphere at 37 °C in DMEM medium supplemented with 10% (v/v) FCS, 10 U/mL penicillin and 10  $\mu\text{g/mL}$  streptomycin. The  $\text{EC}_{50}$  were determined from dose–response assays at seven experimental concentrations (from 200 to 0.001  $\mu\text{M}$ ) of compounds tested in triplicate and essentially as described in Demoro et al.<sup>48</sup>, except that 200  $\mu\text{L}$  of a cell suspension at  $6 \times 10^4$  cells/mL was added per well in a 96-well culture plate. The cytotoxicity was evaluated with a colorimetric assay (WST-1 reagent) that measures the absorbance at 450 nm of the formazan dye produced by metabolically active cells. The photometric measurements were performed with an EL 800 microplate reader (Biotek). The following equation was used to estimate the cytotoxicity: Cytotoxicity (%) =  $\frac{\text{(experimental value} - \text{DMSO control)}}{\text{(growth control} - \text{DMSO control)}} \times 100$ . The data were plotted as percentage cytotoxicity versus compound concentration.  $\text{EC}_{50}$  values were obtained as described above for anti-*T. brucei* activity.

### 5.2.4. Assay for inhibition of mammalian protein kinases

**5.2.4.1. Protein kinase assay buffers.** Buffer A: 10 mM  $\text{MgCl}_2$ , 1 mM EGTA, 1 mM DTT, 25 mM Tris–HCl pH 7.5, 50  $\mu\text{g}$  heparin/mL. Buffer B: 50 mM  $\text{MgCl}_2$ , 90 mM NaCl, 30 mM Tris–HCl pH 7.4.

**5.2.4.2. Kinase preparations and assays.** Kinase activities for each enzyme were assayed in buffer A or B, with their corresponding substrates, in the presence of 15  $\mu\text{M}$  ATP in a final volume of 30  $\mu\text{L}$ . After 30 min incubation at 30 °C, the reaction was stopped by harvesting, using a FilterMate harvester (Packard), onto P81 phosphocellulose papers (GE Healthcare) which were washed in 1% phosphoric acid. Scintillation fluid was added and the radioactivity measured in a Packard counter. Blank values were subtracted and activities calculated as pmoles of phosphate incorporated during the 30 min incubation. The activities were expressed in % of the maximal activity, i.e., in the absence of inhibitors. Controls were performed with appropriate dilutions of DMSO.

*CDK1/cyclin B* (M phase starfish oocytes, native), *CDK2/cyclin A* (human, recombinant, from A. Echalié, University of Leicester), *CDK5/p25* (human, recombinant, expressed in *E. coli*) were assayed in Buffer A (supplemented extemporaneously with 0.15 mg BSA/mL, except for CDK2) with 25 µg of histone H1. *CDK9/cyclin T* (human, recombinant, expressed in insect cells) was assayed as described for CDK1/cyclin B, but using 8.07 µg of CDK7/9-Tide (YSPTSPSYSPSYSPSYSPSKKKK).<sup>49</sup>

*DYRK1A* (human, recombinant, expressed in *E. coli* as a GST fusion protein), and *CLK1* (mouse, recombinant, expressed in *E. coli* as a GST fusion protein) were assayed as described for CDK1/cyclin B with 1 µg of RS peptide (GRSRSRSRSR) as a substrate.<sup>50</sup>

*GSK-3α/β* (porcine brain, native, affinity purified on axin 1-sepharose beads<sup>51</sup>) was assayed as described for CDK1/cyclin B, but using a GSK-3 specific substrate (GS-1: YRRAAVPPSPSLSRHS SPHQpSEDEEE where pS stands for phosphorylated serine).

*Casein kinase 1 (CK1δ/ε)* (porcine brain, native, purified by affinity chromatography on axin 2-sepharose beads<sup>52</sup>) was assayed with 0.67 µg of CKS peptide (RRKHAAGpSAYSITA), a CK1 specific substrate.

### 5.3. In-silico analysis

#### 5.3.1. Modeling

Modeling of FS-554 into the *LmTryS* X-ray structure was performed using MOE [Molecular Operating Environment (MOE), 2013.08; Chemical Computing Group Inc., 1010 Sherbooke St. West, Suite #910, Montreal, QC, Canada, H3A 2R7, 2016]. Due to the lack of available TryS structures in complex with ATP, EcGspS (pdb 2ioa) and GSK-3 (pdb 1j1c) structures with bound ADP were superimposed using MOE and further used as template models. Afterwards, *LmTryS* (2vpm) was structurally superimposed on EcGspS and GSK-3 (pdb 1q3w) in complex with alsterpauillone and on GSK-3 in complex with ADP (pdb 1j1c). Based on this superimposition, alsterpauillone binding coordinates were transferred into the *LmTryS* X-ray structure. The alsterpauillone was modified into FS-554 and after protonation using Protonate3D tool from the MOE package, the *LmTryS* FS-554 complex model was minimized using the 'Energy Minimize' function and the forcefield AmberEHT10 in MOE.

#### 5.3.2. Calculation of predicted LogP values

Predicted LogP values were calculated with ChemBioDraw level Ultra, version 13.02.3021 (CambridgeSoft, PerkinElmer, Cambridge, MA, U.S.A.)

### 5.4. Determination of aqueous solubility

The aqueous solubility was determined by a miniaturized shake-flask-method. In brief, the compound (0.25 mg) was incubated in a Whatman Mini-Uniprep vial with aqueous phosphate buffer, pH 7.4, (500 µL) in an incubation shaker (IKA® KS 3000 ic control, Staufen, Germany) at 25 °C, 400 rpm. Presence of undissolved compound was checked at 12 and 24 h. After 48 h of shaking, the filter plunger was punched into the vial and the concentration in the supernatant was determined by HPLC (AUC method, isocratic HPLC, at specific  $\lambda_{\max}$  as indicated in Section 5.1). For the calibration at least 3 different dilutions of the compounds from DMSO stock solutions diluted with ACN were quantified. Preparation of buffer pH 7.4: To a solution of Na<sub>2</sub>HPO<sub>4</sub>·2H<sub>2</sub>O (290 mg), K<sub>2</sub>HPO<sub>4</sub> (20 mg) and NaCl (808 mg) in water (ad 100.0 mL), 13% aqueous HCl was added drop wise until the pH reached 7.4. In all investigated cases (**3a**, **3f**, **3h**) the concentrations in the supernatant were below the limit of quantification.

Therefore the lowest concentrations used for the calibration are indicated as upper limit of solubility in Table 1.

### Acknowledgements

This project was funded by the German Federal Ministry of Education and Research (BMBF, program KMU-innovativ 5, grant project code 0315814; to R. S. K., O. K., and C. K.) and supported by the COST action CM1307 (to O. C. F. O. and C. K.). The support of FOCEM (MERCOSUR Structural Convergence Fund, COF 03/11), Institut Pasteur ACIP call 2015 (project ACIP 17-2015) and ANII – Uruguay (POS\_NAC\_2013\_1\_114477) is acknowledged by M.A.C., D.B. and A. M., L.M. was supported by a grant from the 'Agence Nationale de la Recherche' (ANR), Transleish. Molecular graphics were performed with the UCSF Chimera package. Chimera is developed by the Resource for Biocomputing, Visualization, and Informatics at the University of California, San Francisco (supported by NIGMS 9P41GM103311). All funding sources were not involved in study design, collection, analysis and interpretation of data; in the writing of the paper; and in the decision to submit the article for publication.

### References and notes

- WHO. *Neglected Tropical Diseases*: <[http://www.who.int/neglected\\_diseases/diseases/en/](http://www.who.int/neglected_diseases/diseases/en/)> (accessed May 29, 2015).
- Chakravarty, J.; Sundar, S. J. *Global Infect. Dis.* **2010**, *2*, 167.
- Lira, R.; Sundar, S.; Makharia, A.; Kenney, R.; Gam, A.; Saraiva, E.; Sacks, D. J. *Infect. Dis.* **1999**, *180*, 564.
- Njoroge, M.; Njuguna, N. M.; Mutai, P.; Ongarora, D. S.; Smith, P. W.; Chibale, K. *Chem. Rev.* **2014**, *114*, 11138.
- Nagle, A. S.; Khare, S.; Kumar, A. B.; Supek, F.; Buchynskyy, A.; Mathison, C. J.; Chennamaneni, N. K.; Pendem, N.; Buckner, F. S.; Gelb, M. H.; Molteni, V. *Chem. Rev.* **2014**, *114*, 11305.
- Comini, M.; Menge, U.; Flohé, L. *Biol. Chem.* **2003**, *384*, 653.
- Comini, M. A.; Menge, U.; Wissing, J.; Flohé, L. *J. Biol. Chem.* **2005**, *280*, 6850.
- Oza, S. L.; Ariyanayagam, M. R.; Aitcheson, N.; Fairlamb, A. H. *Mol. Biochem. Parasitol.* **2003**, *131*, 25.
- Oza, S. L.; Shaw, M. P.; Wyllie, S.; Fairlamb, A. H. *Mol. Biochem. Parasitol.* **2005**, *139*, 107.
- Oza, S. L.; Tetaud, E.; Ariyanayagam, M. R.; Warnon, S. S.; Fairlamb, A. H. *J. Biol. Chem.* **2002**, *277*, 35853.
- Saudagar, P.; Dubey, V. K. *Biol. Chem.* **2011**, *392*, 1113.
- Tetaud, E.; Manai, F.; Barrett, M. P.; Nadeau, K.; Walsh, C. T.; Fairlamb, A. H. *J. Biol. Chem.* **1998**, *273*, 19383.
- Koch, O.; Cappel, D.; Nocker, M.; Jäger, T.; Flohé, L.; Sotriffer, C.; Selzer, P. M. *PLoS One* **2013**, *8*, e56788.
- Fyfe, P. K.; Oza, S. L.; Fairlamb, A. H.; Hunter, W. N. *J. Biol. Chem.* **2008**, *283*, 17672.
- Leroux, A. E.; Haanstra, J. R.; Bakker, B. M.; Krauth-Siegel, R. L. *J. Biol. Chem.* **2013**, *288*, 23751.
- Ariyanayagam, M. R.; Oza, S. L.; Guthrie, M. L.; Fairlamb, A. H. *Biochem. J.* **2005**, *391*, 425.
- Comini, M. A.; Guerrero, S. A.; Haile, S.; Menge, U.; Lünsdorf, H.; Flohé, L. *Free Radic. Biol. Med.* **2004**, *36*, 1289.
- Wyllie, S.; Oza, S. L.; Patterson, S.; Spinks, D.; Thompson, S.; Fairlamb, A. H. *Mol. Microbiol.* **2009**, *74*, 529.
- Sousa, A. F.; Gomes-Alves, A. G.; Benitez, D.; Comini, M. A.; Flohe, L.; Jaeger, T.; Passos, J.; Stuhlmann, F.; Tomas, A. M.; Castro, H. *Free Radic. Biol. Med.* **2014**, *73*, 229.
- Benitez, D.; Medeiros, A.; Fiestas, L.; Panozzo-Zenere, E. A.; Maiwald, F.; Prousis, K. C.; Roussaki, M.; Calogeropoulou, T.; Detsi, A.; Jaeger, T.; Šarlauskas, J.; Mašić, L. P.; Kunick, C.; Labadie, G. R.; Flohé, L.; Comini, M. A. *PLoS Negl. Trop. Dis.* **2016**, *10*.
- Lyssiotis, C. A.; Foreman, R. K.; Staerk, J.; Garcia, M.; Mathur, D.; Markoulaki, S.; Hanna, J.; Lairson, L. L.; Charette, B. D.; Bouchez, L. C.; Bollong, M.; Kunick, C.; Brinker, A.; Cho, C. Y.; Schultz, P. G.; Jaenisch, R. *Proc. Natl. Acad. Sci. U.S.A.* **2009**, *106*, 8912.
- Stukenbrock, H.; Musmann, R.; Geese, M.; Ferandin, Y.; Lozach, O.; Lemcke, T.; Kegel, S.; Lomow, A.; Burk, U.; Dohrmann, C.; Meijer, L.; Austen, M.; Kunick, C. J. *Med. Chem.* **2008**, *51*, 2196.
- Tolle, N.; Kunick, C. *Curr. Top. Med. Chem.* **2011**, *11*, 1320.
- McGrath, C. F.; Pattabiraman, N.; Kellogg, G. E.; Lemcke, T.; Kunick, C.; Sausville, E. A.; Zaharevitz, D. W.; Gussio, R. *J. Biomol. Struct. Dyn.* **2005**, *22*, 493.
- Pies, T.; Schaper, K.-J.; Leost, M.; Zaharevitz, D. W.; Gussio, R.; Meijer, L.; Kunick, C. *Arch. Pharm. Pharm. Med. Chem.* **2004**, *337*, 486.
- Wiekling, K.; Knockaert, M.; Leost, M.; Zaharevitz, D. W.; Meijer, L.; Kunick, C. *Arch. Pharm. Pharm. Med. Chem.* **2002**, *335*, 311.

27. Kunick, C.; Lauenroth, K.; Leost, M.; Meijer, L.; Lemcke, T. *Bioorg. Med. Chem. Lett.* **2004**, *14*, 413.
28. Leost, M.; Schultz, C.; Link, A.; Wu, Y.-Z.; Biernat, J.; Mandelkow, E.-M.; Bibb, J. A.; Snyder, G. L.; Greengard, P.; Zaharevitz, D. W.; Gussio, R.; Senderowicz, A. M.; Sausville, E. A.; Kunick, C.; Meijer, L. *Eur. J. Biochem.* **2000**, *267*, 5983.
29. Schultz, C.; Link, A.; Leost, M.; Zaharevitz, D. W.; Gussio, R.; Sausville, E. A.; Meijer, L.; Kunick, C. *J. Med. Chem.* **1999**, *42*, 2909.
30. Bain, J.; Plater, L.; Elliott, M.; Shpiro, N.; Hastie, C. J.; McLauchlan, H.; Klevernick, I.; Arthur, J. S.; Alessi, D. R.; Cohen, P. *Biochem. J.* **2007**, *408*, 297.
31. Egert-Schmidt, A.-M.; Dreher, J.; Dunkel, U.; Kohfeld, S.; Preu, L.; Weber, H.; Ehlert, J. E.; Mutschler, B.; Totzke, F.; Schächtele, C.; Kubbutat, M. H. G.; Baumann, K.; Kunick, C. *J. Med. Chem.* **2010**, *53*, 2433.
32. Bertrand, J. A.; Thieffine, S.; Vulpetti, A.; Cristiani, C.; Valsasina, B.; Knapp, S.; Kalisz, H. M.; Flocco, M. J. *Mol. Biol.* **2003**, *333*, 393.
33. Kunick, C.; Lauenroth, K.; Wieking, K.; Xie, X.; Schultz, C.; Gussio, R.; Zaharevitz, D.; Leost, M.; Meijer, L.; Weber, A.; Jorgensen, F. S.; Lemcke, T. *J. Med. Chem.* **2004**, *47*, 22.
34. Maiwald, F.; Benítez, D.; Charquero, D.; Dar, M. A.; Erdmann, H.; Preu, L.; Koch, O.; Hölscher, C.; Loaëc, N.; Meijer, L.; Comini, M. A.; Kunick, C. *Eur. J. Med. Chem.* **2014**, *83*, 274.
35. Ghose, A. K.; Herberich, T.; Pippin, D. A.; Salvino, J. M.; Mallamo, J. P. *J. Med. Chem.* **2008**, *51*, 5149.
36. Denis, J. G.; Franci, G.; Altucci, L.; Aurrecochea, J. M.; de Lera, A. R.; Alvarez, R. *Org. Biomol. Chem.* **2015**, *13*, 2800.
37. Saget, T.; Cramer, N. *Angew. Chem., Int. Ed.* **2013**, *52*, 7865.
38. Soto, S.; Vaz, E.; Dell'Aversana, C.; Alvarez, R.; Altucci, L.; de Lera, A. R. *Org. Biomol. Chem.* **2012**, *10*, 2101.
39. Tsyshchuk, I. E.; Vorobyeva, D. V.; Peregudov, A. S.; Osipov, S. N. *Eur. J. Org. Chem.* **2014**, *2014*, 2480.
40. Falke, H.; Chaikuad, A.; Becker, A.; Loaëc, N.; Lozach, O.; Abu Jhaisha, S.; Becker, W.; Jones, P. G.; Preu, L.; Baumann, K.; Knapp, S.; Meijer, L.; Kunick, C. *J. Med. Chem.* **2015**, *58*, 3131.
41. Orban, O. C. F.; Korn, R. S.; Unger, L.; Yildiz, A.; Kunick, C. *Molbank* **2015**, M856.
42. Stout, D. M.; Matier, W. L.; Barcelon-Yang, C.; Reynolds, R. D.; Brown, B. S. *J. Med. Chem.* **1983**, *26*, 808.
43. Taylor, M. C.; Kaur, H.; Blessington, B.; Kelly, J. M.; Wilkinson, S. R. *Biochem. J.* **2008**, *409*, 563.
44. Coombs, G. H.; Sanderson, B. E. *Ann. Trop. Med. Parasitol.* **1985**, *79*, 409.
45. Ariyanayagam, M. R.; Oza, S. L.; Mehlert, A.; Fairlamb, A. H. J. *Biol. Chem.* **2003**, *278*, 27612.
46. Krauth-Siegel, R. L.; Comini, M. *Biochim. Biophys. Acta* **2008**, *1780*, 1236.
47. Biebinger, S.; Wirtz, L. E.; Lorenz, P.; Clayton, C. *Mol. Biochem. Parasitol.* **1997**, *85*, 99.
48. Demoro, B.; Sarniguet, C.; Sanchez-Delgado, R.; Rossi, M.; Liebowitz, D.; Caruso, F.; Olea-Azar, C.; Moreno, V.; Medeiros, A.; Comini, M. A.; Otero, L.; Gambino, D. *Dalton Trans.* **2012**, *41*, 1534.
49. Bettayeb, K.; Oumata, N.; Echalièr, A.; Ferandin, Y.; Endicott, J. A.; Galons, H.; Meijer, L. *Oncogene* **2008**, *27*, 5797.
50. Tahtouh, T.; Elkins, J. M.; Filippakopoulos, P.; Soundararajan, M.; Burgy, G.; Durieu, E.; Cochet, C.; Schmid, R. S.; Lo, D. C.; Delhommel, F.; Oberholzer, A. E.; Pearl, L. H.; Carreaux, F.; Bazureau, J. P.; Knapp, S.; Meijer, L. *J. Med. Chem.* **2012**, *55*, 9312.
51. Primot, A.; Baratte, B.; Gompel, M.; Borgne, A.; Liabeuf, S.; Romette, J. L.; Costantini, F.; Meijer, L. *Protein Expr. Purif.* **2000**, *20*, 394.
52. Reinhardt, J.; Ferandin, Y.; Meijer, L. *Protein Expr. Purif.* **2007**, *54*, 101.